



HAL
open science

Isotopic compositions of copper and zinc in plankton from the Mediterranean Sea (MERITE-HIPPOCAMPE campaign): Tracing trophic transfer and geogenic inputs

Sandrine Chifflet, Nicolas Briant, Rémi Freydier, Daniel Araùjo, Marianne Quéméneur, Hana Zouch, Amel Bellaaj-Zouari, François Carlotti, Marc Tedetti

► To cite this version:

Sandrine Chifflet, Nicolas Briant, Rémi Freydier, Daniel Araùjo, Marianne Quéméneur, et al.. Isotopic compositions of copper and zinc in plankton from the Mediterranean Sea (MERITE-HIPPOCAMPE campaign): Tracing trophic transfer and geogenic inputs. *Marine Pollution Bulletin*, 2022, 185 (Part A), pp.114315. 10.1016/j.marpolbul.2022.114315. hal-03865956

HAL Id: hal-03865956

<https://hal.science/hal-03865956v1>

Submitted on 22 Nov 2022

HAL is a multi-disciplinary open access archive for the deposit and dissemination of scientific research documents, whether they are published or not. The documents may come from teaching and research institutions in France or abroad, or from public or private research centers.

L'archive ouverte pluridisciplinaire **HAL**, est destinée au dépôt et à la diffusion de documents scientifiques de niveau recherche, publiés ou non, émanant des établissements d'enseignement et de recherche français ou étrangers, des laboratoires publics ou privés.



Distributed under a Creative Commons Attribution - NonCommercial - NoDerivatives 4.0 International License

1 **Isotopic compositions of Copper and Zinc in plankton from the Mediterranean Sea**
2 **(MERITE-HIPPOCAMPE campaign): tracing trophic transfer and geogenic inputs**

3

4 Sandrine Chifflet^{a*}, Nicolas Briant^b, Rémi Freydier^c, Daniel F. Araújo^b, Marianne
5 Quéméneur^a, Hana Zouch^d, Amel Bellaaj Zouari^d, François Carlotti^a, Marc Tedetti^a

6

7 ^a Aix Marseille Univ., Université de Toulon, CNRS, IRD, MIO UM 110, 13288, Marseille,
8 France

9 ^b Ifremer, CCEM Contamination Chimique des Écosystèmes Marins, F-44000 Nantes, France

10 ^c HSM, Université de Montpellier, CNRS, Montpellier, France

11 ^d Institut National des Sciences et Technologies de la Mer (INSTM), 28, rue 2 mars 1934,
12 Salammbô 2025, Tunisia

13

14 * Corresponding author: sandrine.chifflet@mio.osupytheas.fr

15

16 For submission to Marine Pollution Bulletin Special issue “*Plankton and Contaminants in the*
17 *Mediterranean Sea: Biological pump and interactions from regional to global approaches*”
18 as a full-length research paper

19

20 Revised version

21 05 October 2022

22

23 **Abstract**

24 This study uses Cu and Zn isotope compositions as proxies of sources and metal
25 transfers in the planktonic food web from the Mediterranean Sea. Plankton was collected in
26 spring 2019 in the deep chlorophyll maximum (DCM) along a North-South transect including
27 coastal and offshore zones (MERITE-HIPPOCAMPE campaign). $\delta^{65}\text{Cu}$ and $\delta^{66}\text{Zn}$
28 compositions were determined on four planktonic size fractions from 60 to 2000 μm .
29 Combined $\delta^{65}\text{Cu}$ and $\delta^{66}\text{Zn}$ with geochemical tracers (Ti, POP) showed that geogenic
30 particles were ubiquitous with plankton assemblages. The $\delta^{15}\text{N}$ ecological tracer showed that
31 planktonic food web was enriched in heavy isotopes in the higher trophic levels. $\delta^{65}\text{Cu}$
32 compositions were correlated with picoplankton in the offshore zone, and with zooplankton
33 in the southern coastal zone. *Firmicutes* bacteria were found correlated with $\delta^{66}\text{Zn}$ zones
34 suggesting decomposition of particulate matter at the DCM. These findings suggest that
35 biogeochemical process may impact Cu and Zn isotopy in the planktonic community.

36

37

38 **Keywords:** Mediterranean Sea, planktonic food web, Cu and Zn isotopes, geogenic inputs

39

40

41

42

43

44

45

46

47

48 1. Introduction

49 Plankton is an important gateway for the accumulation and transfer of trace metal into
50 the marine food web (Rossi and Jamet, 2008; Chauvelon et al., 2019). According to their role
51 in biogeochemical cycles, copper (Cu) and zinc (Zn) can be categorized as essential for
52 marine food web. Indeed, both elements serve as co-factors in enzymes of key metabolic
53 pathways. Cu is a key micronutrient that contributes to photosynthesis, denitrification and
54 iron uptake by primary producers in the food web (Peers et al., 2005; Peers and Price, 2006;
55 Zumft and Kroneck, 2007). However, above 10 pM, free dissolved copper (Cu^{2+}) exerts acute
56 toxic effects on phytoplankton (Moffett et al., 1997) which in turn may release organic
57 ligands that strongly complex Cu as an effective detoxification mechanism (Moffett and
58 Brand, 1996; Croot et al., 2000; Rue and Bruland, 2001). Zn containing enzymes are carbonic
59 anhydrases, essential during biomass buildup from reduced carbon and light (Domsic et al.,
60 2008), or alkaline phosphatases for the acquisition of organic phosphorus when phosphate is
61 scarce (Morel and Price, 2003; Shaked et al., 2006; Cox and Saito, 2013). Because the
62 interactions between metal and organisms are numerous and complex, it is still difficult to
63 understand transfers of Cu and Zn in the planktonic food web.

64 The new generation of high-resolution mass spectrometers, such as the multi-collector
65 inductively coupled plasma mass spectrometers (MC-ICP-MS), have allowed measuring
66 accurately isotope compositions of trace metal in natural marine samples (Araújo et al.,
67 2022a). Cu has two stable isotopes, ^{63}Cu and ^{65}Cu , with natural average abundances of 69.17
68 and 30.83%, respectively, while Zn has five stable isotopes, ^{64}Zn , ^{66}Zn , ^{67}Zn , ^{68}Zn , and ^{70}Zn ,
69 with natural average abundances of 48.63, 27.90, 4.10, 18.75, and 0.62%, respectively
70 (Maréchal et al., 1999). In natural ecosystems, the relative abundance of stable isotopes varies
71 according to isotopic fractionation phenomena occurring during biogeochemical processes,
72 between reactants and products, phases or molecules (Wiederhold, 2015). These changes in

73 isotope ratios have proven useful in tracing sources and biogeochemical processes in
74 hydrothermal systems (Larson et al., 2003; Rouxel et al., 2004; Maher and Larson, 2007), ore
75 deposits (Graham et al., 2004; Mason et al., 2005; Lemaitre et al., 2020a) and open ocean
76 (Conway and John, 2014; Conway et al., 2021). In coastal marine ecosystems, these isotopes
77 have been relevant to track metal dispersion and to differentiate the type and nature of
78 particles (natural *versus* anthropogenic, mineral *versus* organic) by river inputs or atmospheric
79 deposition (Araújo et al., 2022a; b).

80 However, the Cu and Zn isotopic fractionation related to planktonic organisms,
81 colloids and the dissolved matrix in seawater is not yet clearly elucidated. Cu speciation is
82 dominated by Cu²⁺ complexation with organic ligands (Coale and Bruland, 1988; Moffett et
83 al., 1990) and induces a significant isotopic fractionation ($\Delta^{65}\text{Cu}_{\text{complex-free}}$ ranging from +0.1
84 to +0.8‰) during equilibrium exchanges between organically complexed and free inorganic
85 dissolved Cu (Bigalke et al., 2010; Fujii et al., 2013; Ryan et al., 2014). Zn bound to organic
86 ligands exhibits an isotopic fractionation ($\Delta^{66}\text{Zn}_{\text{cell-sw}}$) ranging from -0.8 to -0.2‰ depending
87 on homeostasis pathways during phytoplankton photosynthesis (John et al., 2007a; Peel et al.,
88 2009; John and Conway, 2014). While many studies have investigated the magnitude of Cu
89 and Zn isotopic fractionations under controlled laboratory conditions, few field studies
90 applied these insights to constrain the transfer mechanisms of the elements in real
91 environmental conditions.

92 The Mediterranean Sea is a semi-enclosed sea that covers ~ 0.7% of the total ocean
93 surface area (~ 0.25% by volume), contains 4 to 18% of the world's marine diversity (Bianchi
94 and Morri, 2000; UNEP/MAP-RAC-SPA, 2008) and is characterized by oligotrophic
95 conditions due to its low content in nutrient (The Mermex group, 2011; Marañón et al., 2021).
96 The Mediterranean Sea is subject to natural and anthropogenic exogenous chemical
97 substances coming from rivers, effluents and atmospheric deposition (Guieu et al., 2002;

98 [Heimbürger et al., 2010, 2011](#); [Pey et al., 2010](#); [Llamas-Dios et al., 2021](#); [Desboeufs et al.,](#)
99 [2022](#)). Important changes have been observed in recent decades in small pelagic fish
100 populations of the northwestern Mediterranean Sea related to various environmental factors
101 ([Coll et al., 2019](#)). Multiple drivers including climatic (temperature, UV irradiance),
102 acidification, demersal fishing, ship traffic and coastal pollution would affect 20% of the
103 entire basin and 60–99% of the territorial waters of EU member states of the Mediterranean
104 and Black Seas ([Micheli et al., 2013](#)). Among the pollutants, trace metals are a recurrent
105 concern ([Luy et al., 2012](#)).

106 In order to further understand the biogeochemical cycles of Cu and Zn in the
107 Mediterranean Sea, isotopic compositions of these elements were determined within the
108 planktonic food web (from bacteria to zooplankton) according to three Mediterranean
109 geographical areas: the northern and southern coastal zones, and the offshore zone. Based on
110 these geographical areas, we aim thus to identify geogenic (natural and anthropogenic mineral
111 sources) and biological (planktonic sources) fingerprints and to evidence their underlying
112 biogeochemical processes. The abundance, diversity and taxonomy of plankton assemblages
113 (bacterio-, phyto-, and zoo-plankton) are presented as companion papers ([Quéméneur et al.,](#)
114 [2022](#); [Bellaaj Zouari et al., 2022](#); [Fierro-González et al., 2022](#)) and are used in this study to
115 support the discussion.

116

117

118 **2. Materials and methods**

119 *2.1. Study zone and sampling procedure*

120 The MERITE-HIPPOCAMPE campaign was conducted on the R/V *Antea* ([Tedetti and](#)
121 [Tronczynski, 2019](#)) in spring 2019 along a north-south Mediterranean transect, between the
122 French (Toulon and Marseille, northwestern Mediterranean Sea) and Tunisian coastal zones

123 (Gulf of Gabès, southeastern Mediterranean Sea) according to two legs and ten sampling
124 stations (Table 1). Leg 1 was carried out between April 13th and 28th with sampling of 5
125 stations (St2, St4, St3, St10 and St11; in this chronological order) during the transect from La
126 Seyne-sur-mer to Tunis. Leg 2 was carried out between April 30th and May 14th with
127 sampling of 5 stations (St19, St17, St15, St9, St1; in this chronological order) during the
128 return transect from the Gulf of Gabès to La Seyne-sur-mer (Fig. 1; Table 1). Sampling
129 strategy implied a wide spatio-temporal variability between stations. They were chosen
130 according to different criteria of physical, biogeochemical and biological conditions (Tedetti
131 et al., 2022). We divided the transect in three geographical areas: i) the northern coastal zone
132 (St1 to St4), located in the bays of Toulon and Marseille, ii) the southern coastal zone (St15,
133 St17 and St19), located along the Tunisian coasts and iii) the offshore zone (St9 to St11),
134 located in near the northern zone of the Balearic Thermal Front (St9 and St10), and in the
135 Algerian ecoregion (St11).

136 At each station, a Multiple Horizontal Plankton Sampler (Midi type, Hydro-Bios[®]),
137 referred to hereafter as “MultiNet”, was deployed to collect horizontally plankton in the deep
138 chlorophyll maximum (DCM; Table 1). In a clean lab-container, recovered plankton was
139 fractionated into four size fractions (F3: 60–200 µm, F4: 200–500 µm, F5: 500–1000 µm and
140 F6: 1000–2000 µm) using nylon sieves by wet-sieving with seawater previously filtered
141 through a glass fibre filter (GF/F, Whatman[®]). The four plankton size fractions were
142 partitioned for various analyses (Tedetti et al., 2022) and aliquots for trace metal and isotopic
143 analysis were transferred into pre-cleaned (HCl, 10%) polycarbonate jars and stored at -20 °C.

144

145 2.2. Analytical procedures

146 2.2.1. Elemental concentrations

147 The sample processing was carried out in a trace metal clean laboratory (ISO 5), using
148 high purity acids (Optima grade, Fisher), and ultrapure water (Milli-Q® EQ 7000, Millipore).
149 Planktonic samples (~200 mg dw) were digested in PFA vials (Savillex) with 5 mL of a
150 mixture of pure acids (HF, 0.5 mL; HNO₃, 4.5 mL), heated on a hot-block (120 °C, 24 h),
151 evaporated to near dryness, and re-dissolved in 3 mL of HNO₃ (10%). The digested samples
152 were then diluted using HNO₃ (2%) before running the trace metal analyses. Elemental
153 analyses were performed by an inductively-coupled plasma mass spectrometer (ICP-MS;
154 ICAP-Q™; ThermoScientific®) at the Laboratoire de Biogéochimie des Contaminants
155 Métalliques (LBCM, Ifremer, Nantes). Details of laboratory and analytical procedures
156 concerning trace metal analyses were described in a companion paper ([Chifflet et al., 2022](#)).

157

158 *2.2.2. Chromatographic separation*

159 Prior to isotopic analyses, Cu and Zn were separated from the digested samples by ion
160 exchange chromatography according to the following modified protocol ([Borrok et al., 2007](#)).
161 All critical laboratory equipment (PFA vials, micropipette tips, columns and PFA storage
162 bottles) were acid cleaned before use. Separations were performed under a free-metal laminar
163 flow hood installed in the clean laboratory (ISO 5). Aliquots of digested samples containing ~
164 1000 ng of Cu were evaporated in PFA vials and re-dissolved in 1 mL HCl (10 M). Columns
165 were loaded with 2 mL of pre-cleaned AG-MP1 anion exchange resin (100–200 mesh, Bio-
166 Rad®), rinsed with 10 mL H₂O and conditioned with 10 mL HCl (10 M). Samples were
167 loaded onto the columns and rinsed with 5 mL HCl (10 M) to elute the matrix. Then, Cu
168 fractions were eluted with 20 mL HCl (5 M) followed by Zn fractions with 15 mL HCl (0.01
169 M). All steps were repeated 3 times to complete purification of Cu and Zn. The analyte
170 content recoveries (100 ± 10%) and presence of interfering elements (Ba, Ca, Cr, Mg, Na, Ni,
171 Ti, V) in Cu and Zn fractions were checked by ICP-MS (ICAP-Q™; ThermoScientific) to

172 assure no bias effect on isotope measurements (Maréchal and Albarède, 2002; Petit et al.,
173 2008; Schleicher et al., 2020). Procedural blanks were below 1% of Zn and Cu mass contents
174 in fractions. After purification, Cu and Zn fractions were near-dried and re-dissolved in HNO₃
175 for isotope ratio measurements.

176

177 2.2.3. Isotopic analysis

178 Cu and Zn isotopic compositions were measured by MC-ICP-MS (Neptune Plus™;
179 ThermoScientific) in low mass resolution mode using a SIS (Stable Introduction System)
180 nebulization chamber and a low flow PFA self-aspiration nebulizer. Cu isotopes (⁶³Cu, ⁶⁵Cu)
181 were measured at the PSO platform (Ifremer, Brest). Cu fractions were dissolved at 250 µg/L
182 in HNO₃ (2%, v/v) and introduced at 50 µL/min. Zinc isotopes (⁶⁴Zn, ⁶⁶Zn, ⁶⁷Zn, ⁶⁸Zn) were
183 measured at the AETE-ISO platform (OSU-OREME university, Montpellier). Zn fractions
184 were dissolved at 250 µg/L in HNO₃ (1%, v/v) and introduced at 70 µL/min. Zinc isotopes
185 (⁶⁴Zn, ⁶⁶Zn, ⁶⁷Zn, ⁶⁸Zn), Cu isotopes (⁶³Cu, ⁶⁵Cu) and Ni isotope (⁶²Ni) were monitored
186 simultaneously and ⁶²Ni was used to correct possible isobaric ⁶⁴Ni interferences on ⁶⁴Zn.

187 Instrumental mass fractionation was corrected as described by Bermin et al. (2006)
188 and Zhao et al. (2014). For the Cu isotope analyses, a Zn internal standard (Zn_{ETH}) was added
189 to the purified Cu fractions and a mixture of external standards (Cu_{SRM976} + Zn_{ETH}) was run
190 with a standard bracketing sequence. The mass bias correction on the ⁶⁵Cu/⁶³Cu ratio was
191 performed combining the internal and external normalization using Zn isotopes ratios
192 (⁶⁶Zn/⁶⁴Zn, ⁶⁷Zn/⁶⁴Zn, ⁶⁸Zn/⁶⁴Zn, and ⁶⁸Zn/⁶⁶Zn) and an exponential law correction. The final
193 Cu isotopic compositions (δ⁶⁵Cu) were reported relative to NIST SRM976 as follow (Eq.1):

$$194 \quad \delta^{65} Cu_{SRM976}(\text{‰}) = \left(\frac{\left(\frac{^{65}Cu}{^{63}Cu} \right)_{sample}}{\left(\frac{^{65}Cu}{^{63}Cu} \right)_{SRM\ 976}} - 1 \right) \times 1000 \quad (\text{Eq. 1})$$

195 For the Zn isotope analyses, a Cu internal standard (Cu_{SRM976}) was added to the purified Zn
 196 fractions and the mixture of external standards (Cu_{SRM976} + Zn_{ETH}) was unchanged. Due to the
 197 depletion of the Zn standard (Zn_{JMC-Lyon}), we replaced this latter by a new reference standard
 198 (Zn_{ETH}). However, we chose to express our $\delta^{66}\text{Zn}$ values relative to JMC-Lyon in order to
 199 compare our data with the literature (Araújo et al., 2017). Therefore, the $\delta^{66}\text{Zn}_{\text{ETH}}$ values were
 200 converted to $\delta^{66}\text{Zn}_{\text{JMC-Lyon}}$ values by adding a factor of 0.28‰ as recommended by Archer et
 201 al. (2017). The final Zn isotopic compositions ($\delta^{66}\text{Zn}$) relative to JMC-Lyon were expressed
 202 as follow (Eq. 2):

$$203 \quad \delta^{66}\text{Zn}_{\text{JMC-Lyon}}(\text{‰}) = \left(\frac{\left(\frac{{}^{66}\text{Zn}}{{}^{64}\text{Zn}} \right)_{\text{sample}}}{\left(\frac{{}^{66}\text{Zn}}{{}^{64}\text{Zn}} \right)_{\text{ETH}}} - 1 \right) \times 1000 + 0.28 \quad (\text{Eq. 2})$$

204 External precision (2σ) was obtained from repeated (2 to 3) measurements of samples.
 205 Long-term precision was assessed from plankton certified materials (BCR 414). The
 206 $\delta^{65}\text{Cu}_{\text{BCr414}}$ ($-0.13 \pm 0.12\text{‰}$; n=2) agreed with reported values in literature ($-0.29 \pm 0.10\text{‰}$;
 207 Yang et al., 2020; $-0.27 \pm 0.05\text{‰}$; Takano et al., 2020). The $\delta^{66}\text{Zn}_{\text{BCr414}}$ ($+0.42 \pm 0.04\text{‰}$; n=2)
 208 fell in the same range of published recommended value ($+0.36 \pm 0.10\text{‰}$; Druce et al., 2020)
 209 and agreed with reported values in literature ($+0.42 \pm 0.04\text{‰}$; Maréchal et al., 2002).

210

211 2.2.4. Isotopic analysis

212 Freeze-dried samples were ground to fine powder with an agate mortar and pestle.
 213 Approximately 0.5 mg of powder was weighed into a tin cup (8×5 mm) using a precision
 214 balance ($d = 0.00001$ g). N isotopic compositions were measured using elemental analyzer
 215 mass spectrometer Integra CN Sercon (Raimbault et al., 2008; Lacoste et al., 2016). N
 216 isotopes (^{14}N , ^{15}N) were carried out at the PACEM platform (Mediterranean Institute of
 217 Oceanography, Marseilles). The $\delta^{15}\text{N}$ composition was reported relative to conventional
 218 standard (atmospheric N_2) as follow (Eq. 3):

$$\delta^{15}\text{N}_{\text{N}_2}(\text{‰}) = \left(\frac{\left(\frac{^{15}\text{N}}{^{14}\text{N}} \right)_{\text{sample}}}{\left(\frac{^{15}\text{N}}{^{14}\text{N}} \right)_{\text{N}_2}} - 1 \right) \times 1000 \quad (\text{Eq. 3})$$

External precision (0.5 ‰) was obtained from repeated (2 to 3) measurements of samples.

221

2.3. Data processing

2.3.1. Biotic trace metal concentration

Marine particles are composed of complex assemblages of biotic (e.g., organic matter from living and dead organisms) and geogenic (e.g., minerals from natural and anthropogenic sources) components (Jeandel et al., 2015; Lam et al., 2018). The relative contribution of the latter component depends on the proximity and intensity of sources. In the field, the separation between biotic and geogenic particles remains an operationally challenging and requires an ultra-clean environment and specific equipment to avoid contaminations (Cullen and Sherrell, 1999; Plaquette and Sherrell, 2012).

However, using normalized ratios of particulate organic phosphorus (P-normalization), a biotic component equated to the fraction of organic matter can be estimated in marine particles (Ho et al., 2007; Liao et al., 2017).

$$[M]_{\text{sample}} = b \cdot [\text{POP}]_{\text{b}} + a \cdot [\text{Ti}]_{\text{a}} \quad (\text{Eq. 4})$$

$$\frac{[M]_{\text{sample}}}{[\text{Ti}]_{\text{sample}}} \equiv b \cdot \frac{[\text{POP}]_{\text{sample}}}{[\text{Ti}]_{\text{sample}}} + a \quad (\text{Eq. 5})$$

where a is Ti-normalized elemental ratio in the geogenic component, b is P-normalized elemental ratio in the biotic component, $[M]_{\text{sample}}$ is elemental concentration in the sample, $[\text{Ti}]_{\text{a}}$ is Ti concentration in the geogenic component, and $[\text{POP}]_{\text{b}}$ is concentration of particulate organic phosphorus in the biotic component. Assuming that POP and Ti in samples are mainly due to the biotic and geogenic components, respectively ($[\text{POP}]_{\text{sample}} \equiv [\text{POP}]_{\text{b}}$;

241 $[\text{Ti}]_{\text{sample}} \equiv [\text{Ti}]_{\text{a}}$), we can turn the mass balance formula into a first-order equation (Eq. 5) and
242 resolved the model.

243 This technique has been extensively detailed by Chifflet et al. (2022) as companion
244 paper and results (biotic, %) are summarized in Table 2.

245

246 2.3.2. Statistical analyses

247 Spearman correlation analyses were performed to identify relations between
248 environmental variables using Xlstat software package version 2019.1.1 (Addinsoft 2020,
249 Boston, USA, <https://www.xlstat.com>). A principal component analysis (PCA) was carried out
250 to extract the key biological factors driving Cu and Zn isotopic composition based on the
251 Spearman correlation test, with a statistical significance level higher than 95% ($p < 0.05$). It
252 was performed using the abundance of bacterial, phytoplanktonic and zooplanktonic
253 communities identified in samples and associated Cu, Zn isotope compositions.

254

255

256 3. Results and discussion

257 3.1. Cu and Zn isotopic composition in plankton

258 In the present study, isotopic compositions ($\delta^{65}\text{Cu}$ and $\delta^{66}\text{Zn}$) in samples are explored
259 in relation to their respective concentrations (Cu and Zn) in four particles size fractions (F3:
260 60–200 μm , F4: 200–500 μm , F5: 500–1000 μm and F6: 1000–2000 μm) collected into the
261 DCM in order to better understand the biogeochemical cycles of Cu and Zn within the
262 Mediterranean planktonic food web (Fig. 2; Table 3). Note that some samples (*i.e.*, St1-F3
263 and St1-F6) had too little amount of Cu and Zn (< 1000 ng) to perform isotopic analysis,
264 which explains some missing data in Table 3. All other data of the MERITE-HIPPOCAMPE
265 campaign for trace metal (As, Cd, Cr, Cu, Fe, Mn, Ni, Sb, Ti, V, Zn) and associated

266 particulate organic phosphorus (POP) in the four size fractions are detailed in a companion
267 paper (Chifflet et al., 2022).

268 The Cu isotopic composition ($\delta^{65}\text{Cu}$) in the different stations and planktonic size
269 fractions (60–2000 μm) ranged from +0.05 to +1.23‰ and was isotopically heavier than the
270 particulate fraction (-0.03 to +0.54‰; 0.8-51 μm ; Little et al., 2018) and marine aerosols
271 (+0.00 to +0.18‰; Little et al., 2014) measured in the South Atlantic. The Zn isotopic
272 composition ($\delta^{66}\text{Zn}$) in the different stations and planktonic size fractions (60–2000 μm) was
273 relatively narrower, varying from +0.33 to +0.59‰. It was also isotopically heavier than
274 $\delta^{66}\text{Zn}$ measured in marine particles of the central Atlantic Ocean (+0.15 to +0.43‰; Maréchal
275 et al., 2000). It should be noticed that the MERITE-HIPPOCAMPE campaign was conducted
276 in spring and, an increase of $\delta^{66}\text{Zn}$ values was already observed during bloom events in
277 oceanic waters (Maréchal et al., 1998) as well as in lacustrine systems (Peel et al., 2009). A
278 general examination of data did not allow to identify any clear trend between $\delta^{65}\text{Cu}$ and $\delta^{66}\text{Zn}$
279 and their respective concentrations (Cu and Zn), neither as a function of spatial distribution,
280 nor as a function of size fractions (Fig. S1 as supplementary information).

281 The distribution of trace metal in planktonic food web is driven by complex
282 biogeochemical cycles (Collier and Edmond, 1984; Bruland and Lohan, 2003; Sunda, 2012).
283 As micronutrients, Cu and Zn are essential to phytoplankton activities through photosynthesis
284 processes and construction of macromolecules (Morel et al., 2008). Then, trace metal are
285 transferred into the trophic food web through dietary pathway (Sun et al., 2020). Besides
286 biological processes, geogenic particles issued from rivers, effluents and atmospheric
287 deposition (Radakovich et al., 2008; Oursel et al., 2013) may contribute to the $\delta^{65}\text{Cu}$ and
288 $\delta^{66}\text{Zn}$ signatures found in plankton. Hence, the $\delta^{65}\text{Cu}$ and $\delta^{66}\text{Zn}$ fingerprint observed here in
289 the different planktonic size fractions may result from both biological/trophic transfer
290 processes and geogenic inputs, the discrimination between the two remaining technically

291 challenging (Cullen and Sherrell, 1999; Cloquet et al., 2008; Plaquette and Sherrell, 2012;
292 [Bacconnais et al., 2019](#)).

293

294 *3.2. Geogenic contribution on Cu and Zn isotopic compositions in plankton*

295 Geogenic particles (*i.e.* minerals from natural and anthropogenic sources) are
296 ubiquitous and enter in marine ecosystems through various processes such as weathering,
297 atmospheric deposition, sediment resuspension ([Bianchi, 2007](#)). The variations of $\delta^{65}\text{Cu}$ and
298 $\delta^{66}\text{Zn}$ in geogenic particles are greater than 1‰ and encompass multiple natural and
299 anthropogenic sources ([Fig. 3](#)). For example, in the natural soil, due to the large variability of
300 geological zones, $\delta^{65}\text{Cu}$ and $\delta^{66}\text{Zn}$ vary widely from -0.15 to +0.44‰ and from -0.03 to
301 +0.43‰, respectively ([Fekiacova et al., 2015](#)). Similar variations are also found in Saharan
302 dusts ($\delta^{65}\text{Cu} = -0.01 \pm 0.14\text{‰}$ and $\delta^{66}\text{Zn} = +0.19 \pm 0.15\text{‰}$; [Schleicher et al., 2020](#)) or marine
303 particles ($\delta^{65}\text{Cu} = +0.23 \pm 0.20\text{‰}$; [Little et al., 2018](#) and $\delta^{66}\text{Zn} = +0.35 \pm 0.08\text{‰}$; [Maréchal et](#)
304 [al., 2002](#)). Based on a compilation of results from basaltic and ultramafic samples from
305 different geological zones, the isotopic fingerprint of Cu and Zn in a bulk silicate earth (BSE)
306 can be estimated as $\delta^{65}\text{Cu} = +0.06 \pm 0.20\text{‰}$ and $\delta^{66}\text{Zn} = +0.28 \pm 0.05\text{‰}$ ([Chen et al., 2013](#);
307 [Liu et al., 2015](#)). However, establishing a natural baseline seems difficult to achieve because
308 similar $\delta^{65}\text{Cu}$ and $\delta^{66}\text{Zn}$ can also be found in other natural particles such as carbonates ($\delta^{66}\text{Zn}$
309 = $+0.73 \pm 0.41\text{‰}$; [Fekiacova et al., 2015](#)), Fe-Mn nodules ($\delta^{65}\text{Cu} = +0.31 \pm 0.23\text{‰}$ and $\delta^{66}\text{Zn}$
310 = $+0.90 \pm 0.28\text{‰}$; [Maréchal et al., 2000](#)), chalcopyrite ($\delta^{65}\text{Cu} = -1.91 \pm 2.50\text{‰}$; [Mathur et al.,](#)
311 [2005; 2014](#)) and sphalerite ($\delta^{66}\text{Zn} = +0.17 \pm 0.20\text{‰}$; [Sonke et al., 2008](#)).

312 The artificial anthropogenic processes, such as ore refining and electrolysis, can also
313 fractionate isotopes leading to fingerprints in byproducts distinguishable from natural
314 background. Redox processes can induce Cu isotopic fractionation, whereby Cu^{II} -bound
315 products are enriched in heavier isotopes while Cu^{I} -bound products are preferentially

316 composed of lighter isotopes (Ehrlich et al., 2004). As a result, major $\delta^{65}\text{Cu}$ variations in
317 anthropogenic reservoirs can be found in pesticides (from -0.49 to +0.89‰; Blotevogel et al.,
318 2018), antifouling paints (Briant et al., 2022), urban aerosol (Souto-Oliviera et al., 2018;
319 2019) and in traffic-related inputs (from -0.18 to +0.71‰ with a median value of +0.34‰;
320 Dong et al., 2017). Due to its low boiling point temperature and high fractionation in
321 evaporation–condensation processes, Zn isotopic fractionation varies widely in coal activities
322 (-0.10 to +1.35‰; Desaully et al., 2020). In addition to contamination from fossil combustion,
323 industrial activities also release Zn particles. For example, $\delta^{66}\text{Zn}$ varies from +0.5 to +1.3‰
324 in metallurgic and electroplating waste (Sirvy et al., 2008; Araújo et al., 2017), from -0.1 to
325 +0.6‰ in non-exhaust traffic emission (Dong et al., 2017), from +0.11 to +0.71‰ in
326 galvanized hardware (John et al., 2007b), from +0.38 to +0.76‰ near Pb-Zn smelter (Juillot
327 et al., 2011), from +0.40 to +0.46‰ in ZnO fumes (Shield et al., 2010), and from +0.18 to
328 +0.20‰ in N-fertilizer or +0.40 to +0.44‰ in P-fertilizer (Chen et al., 2008).

329 To assess the potential influence of geogenic particles on Cu and Zn isotopic
330 compositions of Mediterranean plankton, $\delta^{65}\text{Cu}$ and $\delta^{66}\text{Zn}$ variations were examined in
331 relation to Cu/POP and Zn/POP in the four size fractions, according to the three geographical
332 zones (Fig. 4). Two pools of samples stand out. The first pool (Pool 1) was composed of
333 samples with great $\delta^{65}\text{Cu}$ and $\delta^{66}\text{Zn}$ variations (from +0.05 to +1.23‰ and from +0.33 to
334 +0.59‰, respectively) in relation to low Cu/POP and Zn/POP ratios (from 1.1 to 3.4 $\mu\text{g}/\text{mg}$
335 and from 20.9 to 44.9 $\mu\text{g}/\text{mg}$, respectively). The second pool (Pool 2) was composed of
336 samples with lower $\delta^{65}\text{Cu}$ and $\delta^{66}\text{Zn}$ variations (from +0.29 to +0.59‰ and from +0.35 to
337 +0.48‰, respectively) in relation to higher Cu/POP and Zn/POP ratios (from 5.9 to 8.7 $\mu\text{g}/\text{mg}$
338 and from 63.6 to 100.7 $\mu\text{g}/\text{mg}$, respectively).

339 According to our companion paper (Chifflet et al., 2022), samples from Pool 2 seemed
340 dominated by a geogenic component since they samples were poor in organic matter with a

341 biotic component < 40%. Otherwise, the samples from Pool 1 were organic rich with a biotic
342 component ranging from 60 to 100% (Table 2). The Ti is known to be a geogenic element
343 (Ohnemus and Lam, 2015) unaffected by biological uptake or particulate recycling
344 (Dammshäuser et al., 2013). Therefore, Ti/POP ratio can be used to represent geogenic vs
345 biotic particles. While the Cu/POP vs Ti/POP diagram showed clear relationships with
346 samples from the same geographic area, these trends appeared more nuanced with the Zn
347 diagram (Fig. 5). Due to geographic characteristics (distance from shore, bathymetry), waters
348 from the northern and southern coastal zones were very likely more influenced by weathering
349 processes and sediment resuspension than were waters from the offshore zone. The increase
350 of Cu/POP and Ti/POP ratios were concomitant to the relative decrease of the biotic
351 compartment against the geogenic counterpart. The two linear trends observed in the Cu
352 diagram probably represented a ‘geogenic-dilution’ line of the northern and southern coastal
353 zones. Slopes suggest different geogenic sources and outpoints (e.g. St1-F6, St2-F3, St4-F5,
354 St17-F4) could be due to poor separation of plankton size fractions in the field. The offshore
355 values overlap the lower end of the ‘geogenic-dilution’ lines, showing a mixture of geogenic
356 particles in both the northern and southern coastal zones. Different anthropogenic source
357 contributions could explain the different slopes and the isotopic fingerprint overlapping.
358 Therefore, Cu and Zn geogenic sources could not be identified precisely in our samples. On-
359 board particle sieving could not be as selective as expected and geogenic particles may have
360 remained “stuck” or accumulated with some fractions when washing was not performed
361 optimally.

362

363 *3.3. Effects of the trophic transfer and homeostasis on Cu and Zn isotopic compositions*

364 Cu and Zn isotopic compositions increased with $\delta^{15}\text{N}$, indicating an enrichment in
365 heavy isotopes in the higher trophic levels (Fig. 6). Only samples from the southern coastal

366 zone did not follow this pattern. The trophic Cu and Zn isotope fractionation has been already
367 studied in mammals from terrestrial and marine environments (Jaouen et al., 2013; Araújo et
368 al., 2021), but isotope patterns in marine food webs remain unknown so far. Despite this gap,
369 it is recognized that speciation, uptake mechanisms and metabolism are key parameters
370 controlling trophic isotope fractionation in plankton-zooplankton realm.

371 Cu and Zn are essential elements involved in many metabolic mechanisms making it
372 difficult to identify the main biological mechanisms driving their isotopic fractionation in the
373 frame of field studies. Indeed, each metabolic pathway (adsorption, precipitation, redox) can
374 induce isotopic fractionation in favor of one isotope or another. For example, Cu uptake into a
375 biofilm can cause a relative enrichment of ^{65}Cu and Cu uptake across the cell membrane can
376 favor ^{63}Cu (Bigalke et al., 2010; Courtaud et al., 2014). Furthermore, the enzymatic activity
377 involved in $\text{Cu}^{\text{I}}\text{-Cu}^{\text{II}}$ redox processes modifies the Cu fractionation with Cu^{I} species in favor
378 of light isotope (Zhu et al., 2002; Ehrlich et al., 2004; Navarrete et al., 2011; Fujii et al., 2013;
379 Moynier et al., 2017). Similar to Cu, biological processes can also be invoked to explain Zn
380 isotopic composition in the planktonic food web. Previously, ^{66}Zn enrichment in planktonic
381 biomass was found to vary from +0.19 and +0.43‰ depending on species and environmental
382 conditions (Maréchal et al., 2000; Gélabert et al. 2006; John et al. 2007a). In natural
383 environment, the main processes inducing Zn fractionation are adsorption (with organic or
384 inorganic ligands) and diffusion (Cloquet et la., 2008; Coutaud et al., 2014). While Zn
385 adsorption on organic matter and carrier proteins are mechanisms of heavy isotope
386 enrichment in marine organisms (Weiss et al., 2005; Gélabert et al., 2006; John and Conway,
387 2014), diffusion of Zn through the phytoplanktonic cell is preferentially into lighter Zn (John
388 et al., 2007a; Peel et al., 2009; John and Conway, 2014).

389 During the MERITE-HIPPOCAMPE campaign, samples from four size fractions were
390 subsampled for bacterial (Quéméneur et al., 2022), phytoplanktonic (Bellaaj Zouari et al.,

391 2022) and zooplanktonic (Fierro-González et al., 2022) diversity, taxonomy and abundance.
392 Hence, Spearman correlations between $\delta^{65}\text{Cu}$ and $\delta^{66}\text{Zn}$ values and abundances of various
393 bacteria, phytoplankton and zooplankton species were investigated (Table S1 as
394 supplementary information). When considering all stations, significant ($p < 0.05$) but weak
395 correlations ($r < 0.5$) were found for all parameters. However, some discrepancies were
396 observed at regional scale. In the northern coastal zone, $\delta^{66}\text{Zn}$ was strongly correlated with the
397 relative abundance of the phylum *Firmicutes* ($r = 0.81$, $p < 0.05$) (Table S2 as supplementary
398 information), which includes heterotrophic bacteria usually present during decomposition
399 processes in water and sediments (Zhao et al., 2017). In the offshore zone, $\delta^{65}\text{Cu}$ was strongly
400 correlated with *Prochlorococcus sp.*, the phylum *Cyanobacteria* and picoeukaryotes ($r = 0.78$,
401 $p < 0.05$) (Table S3 as supplementary information). In the southern coastal zone, while $\delta^{65}\text{Cu}$
402 and $\delta^{66}\text{Zn}$ were moderately correlated with *Firmicutes* ($r = -0.66$ and 0.57 , $p < 0.05$,
403 respectively), $\delta^{65}\text{Cu}$ was strongly correlated with zooplanktonic organisms, i.e., copepods ($r =$
404 -0.94 , $p < 0.05$) (Table S4 as supplementary information).

405 Under strong anthropogenic pressure, coastal waters receive both large inputs of
406 nutrients that can stimulate phytoplanktonic activities (Cruzado and Velasquez, 1990; Macias
407 et al., 2019) and a cocktail of contaminants that can induce changes in the biodiversity of
408 primary producers (Hulot et al., 2000; Johnston and Roberts, 2009; Goni-Urriza et al., 2018).
409 In such conditions, Cu can reduce copepods eggs production, thus negatively impact primary
410 predator communities (Lauer and Bianchini, 2010). Furthermore, bacteria are known to
411 strongly fractionate Cu ($\Delta^{65}\text{Cu}_{\text{media-cell}}$ from +1.0 to +4.4‰; Navarrete et al., 2010), and lower
412 interactions between bacteria and phytoplankton were already observed by Pringault et al.
413 (2020; 2021) in contaminated Bizerte Lagoon (southeastern Mediterranean Sea, Tunisia). The
414 lower $\delta^{65}\text{Cu}$ values in the southern coastal zones and the strong anti-correlation with copepods
415 could suggest a discrepancy in the southern coastal zone. The impact of Cu in the Gulf of

416 Gabès (southern coastal zone) should be further investigated as a significant transfer of Cu
417 into the planktonic food web was also observed in a companion study (Chifflet et al., 2022).

418

419

420 4. Conclusions

421 In this study, we propose an isotopic approach to examine the Cu and Zn transfers in
422 the planktonic food web in three geographical areas of the Mediterranean Sea: the northern
423 coastal zone (bays of Toulon and Marseille, France), the offshore zone (near the Balearic
424 Thermal Front) and the southern coastal zone (Gulf of Gabès, Tunisia). Overall, geogenic
425 particles were ubiquitous in the different sizes of plankton (60–200, 200–500, 500–1000,
426 1000–2000 μm) and the Cu and Zn isotope compositions seems to reflect a complex mixing
427 of signatures of geogenic (from natural and anthropic sources) and planktonic assemblages.
428 Nevertheless, elemental and isotope Cu-Zn data combined with proxies for geogenic (Ti) and
429 organic matter (POP) indicated that geogenic particles in the northern and southern coastal
430 zone were of different origins, and that in the offshore, geogenic particles were from a
431 mixture of northern and southern sources. The $\delta^{65}\text{Cu}$ and $\delta^{66}\text{Zn}$ variations were examined in
432 relation to $\delta^{15}\text{N}$ and showed trends of heavy isotope enrichment in the planktonic food web
433 from the northern and offshore zones. Discrepancies were observed between the southern
434 coastal zone and the latter two zones. While $\delta^{65}\text{Cu}$ was strongly correlated with
435 *Prochlorococcus sp.* and picoeukaryotes in the offshore zone, $\delta^{65}\text{Cu}$ was strongly correlated
436 with copepods in the southern coastal zone. We suggest that the southern coastal zone
437 exhibits a shift in the community structure due to Cu biogeochemical interactions.
438 Furthermore, the bacterial phylum *Firmicutes* was found correlated with $\delta^{66}\text{Zn}$, suggesting
439 decomposition of particulate matter at the DCM in Mediterranean coastal ecosystems.

440 In the framework of the MERITE-HIPPOCAMPE campaign, a companion study
441 showed amplification of essential and non-essential elements (As, Cu, Cr, Sb) in biotic
442 compartment of southern coastal zones (Chifflet et al., 2022). The present study confirms the
443 impact of trace metal on planktonic food web of the Mediterranean Sea. During the campaign,
444 we encountered challenging weather conditions with winds up to 40 knots and 3 m waves. As
445 a result, collecting and sieving particles on-board was operationally difficult without time for
446 replicates. For future research, we recommend limiting studies to homogeneous geographic
447 areas (same physico-chemical characteristics of waters, same anthropogenic influences) and
448 collecting plankton in size fractions ranging from 0.2 to 2000 μm .

449

450

451

452 ***Authors contribution.*** All the authors participated in the MERITE-HIPPOCAMPE project
453 and contributed to the sampling strategy, preparation of the material, field work, laboratory
454 analyses and/or data processing and interpretation. SC and NB wrote the original manuscript,
455 and all the authors participated to its reviewing and/or editing.

456

457

458 ***Acknowledgments.*** The MERITE-HIPPOCAMPE project was initiated and funded by the
459 “Pollution & Contaminants” transversal axis of the CNRS-INSU MISTRALS program (joint
460 action of the MERMEX-MERITE and CHARMEX subprograms). It has also received the
461 financial support of the Franco-Tunisian International Joint Laboratory (LMI) COSYS-Med.
462 The MERITE-HIPPOCAMPE campaign was organized and supported by the French
463 (Oceanographic Fleet, CNRS/INSU, IFREMER, IRD) and Tunisian institutions (Ministry of
464 Agriculture, Hydraulic Resources and Fisheries of Tunisia, Ministry of Higher Education and

465 Scientific Research of Tunisia). The project has also received additional funding from the
466 MIO's incentive "Action Sud" and "Transverse" programs (CONTAM project) and by the
467 ANR CONTAMPUMP (ANR JCJC #19-CE34-0001-01). We acknowledge the MIO's
468 platforms: "Service Atmosphère-Mer" (SAM) for the preparation and management of the
469 embarked material and, "Plateforme Analytique de Chimie des Environnements Marins"
470 (PACEM), the staff from LBCM-Ifremer laboratory for various chemical analyses and the
471 staff from AETE-ISO platform from the OSU-OREME university for the MC-ICP-MS
472 analyses. The authors are deeply grateful for the thorough and constructive corrections and
473 insightful comments of the anonymous reviewers, who have significantly improved the
474 original manuscript.

475

476

477

478

479 **References**

- 480 Araújo, D.F., Boaventura, G.R., Viers, J., Mulholland, D.S., Weiss, D., Araújo, D., Lima, B.,
481 Ruiz, I., Machado, W., Babinski, M., Dantas, E., 2017. Ion exchange chromatography and
482 mass bias correction for accurate and precise Zn isotope ratio measurements in
483 environmental reference materials by MC-ICP-MS. *J. Braz. Chem. Soc.*, 28, 225–235.
- 484 Araújo, D.F., Ponzevera, E., Briant, N., Knoery, J., Bruzac, S., Sireau, T., Grouhel-Pellouin,
485 A., Brach-Papa, C., 2021. Differences in Copper Isotope Fractionation Between Mussels
486 (Regulators) and Oysters (Hyperaccumulators): Insights from a Ten-Year Biomonitoring
487 Study. *Environ. Sci. Technol.*, 55, 324-330.

488 Araújo, D.F., Knoery, J., Briant, N., Vigier, N., Ponzevera, E., 2022a. “Non-traditional”
489 stable isotopes applied to the study of trace metal contaminants in anthropized marine
490 environments. *Mar. Pollut. Bull.*, 175, 113398.

491 Araújo, D.F., Knoery, J., Briant, N., Ponzevera, E., Mulholland, D.S., Bruzac, S., Sireau, T.,
492 Chouvelon, T., 2022b. Cu and Zn stable isotopes in suspended particulate matter sub-
493 fractions from the northern Bay of Biscay help identify biogenic and geogenic particle
494 pools. *Cont. Shelf Res.*, 244, 104791.

495 Archer, C., Andersen, M.B., Cloquet, C., Conway, T.M., Dong, S., Ellwood, M., Moore, R.,
496 Nelson, J., Rehkämper, M., Rouxel, O., Samanta, M., Shin, K.-C., Sohrin, Y., Takano, S.,
497 Wasylenki, L., 2017. Inter-calibration of a proposed new primary reference standard AA-
498 ETH Zn for zinc isotopic analysis. *J. Anal. At. Spectrom.* 32, 415–419.

499 Baconnais, I., Rouxel, O., Dulaquais, G., Boye, M., 2019. Determination of the copper
500 isotope composition of seawater revisited: a case study from the Mediterranean Sea. *Chem.*
501 *Geol.*, 511, 465-480.

502 Bellaaj Zouari, A., et al., 2022. Analysis of phytoplankton and bacterioplankton variations and
503 structure along a North-south Mediterranean transect. *Mar. Pollut. Bull.*, in prep in this
504 special issue.

505 Bianchi, C.N., Morri, C. 2000. Marine biodiversity of the Mediterranean Sea: situation,
506 problems and prospects for future research. *Mar. Pollut. Bull.*, 40, 367-376.

507 Bianchi, T.S., 2007. *Biogeochemistry of estuaries*. Oxford University Press.

508 Bigalke, M., Weyer, S., Wilcke, W., 2010. Copper Isotope Fractionation during
509 Complexation with Insolubilized Humic Acid. *Environ. Sci. Technol.*, 44, 5496-5502.

510 Blotevogel, S., Oliva, P., Sobanska, S., Viers, J., Vezin, H., Audry, S., Prunier, J., Darrozes,
511 J., Orgogozo, L., Courjault-Radé, P., Schreck, E., 2018. The fate of Cu pesticides in

512 vineyard soils: a case study using $\delta^{65}\text{Cu}$ isotopes ratios and EPR analysis. *Chem. Geol.*,
513 477, 35-46.

514 Borrok, D.M., Wanty, R.B., Ridley, W.I., Wolf, R., Lamothe, P.J., Adams, M., 2007.
515 Separation of copper, iron, and zinc from complex aqueous solutions for isotopic
516 measurement. *Chem. Geol.*, 242, 400-414.

517 Briant, N., Freydier, R., Araújo, D., Delpoux, S., Elbaz-Poulichet, F., 2022. Cu isotope
518 records of Cu-based antifouling paints in sediment core profiles from the largest European
519 Marina, The Port Camargue. *Sci. Tot. Environ.*, 157885.

520 Bruland, K.W., Lohan, M.C., 2003. Control of trace metals in seawater. *Treatise Geom.*, 6,
521 23-47.

522 Chen, J., Gaillardet, J., Louvat, P., 2008. Zinc isotopes in the Seine River waters, France: a
523 probe of anthropogenic contamination. *Environ. Sci. Technol.*, 42, 6494-6501.

524 Chen, H., Savage, P.S., Teng, F.-Z., Helz, R.T., Moynier, F., 2013. Zinc isotope fractionation
525 during magmatic differentiation and the isotopic composition of the bulk earth. *Earth
526 Planet. Sci. Lett.*, 369-370, 34-42.

527 Chifflet, S., Briant, N., Tesán-Onrubia, J.A., Zaaboub, N., Armi, S., Radakovitch, O., Bănaru,
528 D., Tedetti, M., 2022. Distribution and accumulation of metals and metalloids in the
529 planktonic food web of the Mediterranean Sea (MERITE-HIPPOCAMPE campaign). *Mar.
530 Pollut. Bul.*, 185, accepted.

531 Chouvelon, T., Strady, E., Harmelin-Vivien, M., Radakovitch, O., Brach-Papa, C., Crochet, S.,
532 Knoery, J., Rozuel, E., Thomas, B., Tronczynski, J., Chiffolleau, J.F., 2019. Patterns of
533 trace metal bioaccumulation and trophic transfer in a phytoplankton-zooplankton-small
534 pelagic fish marine food web. *Mar. Pollut. Bull.*, 146, 1013-1030.

535 Cloquet, C., Carignan, J, Lehmann, M.F., Vanhaecke, F., 2008. Variation in the isotopic
536 composition of zinc in the natural environment and the use of zinc isotopes in
537 biogeosciences: a review. *Anal. Bioanal. Chem*, 390, 451-463.

538 Coale, K.H., Bruland, K.W., 1988. Copper complexation in the Northeast Pacific. *Limnol.*
539 *Oceanogr.*, 33, 1084-1101.

540 Coll, M., Albo-Puigserver, M., Navarro J., Palomera, I., Dambacher, J.M., 2019. Who is to
541 blame? Plausible pressures on small pelagic fish population changes in the northwestern
542 Mediterranean Sea. *Mar. Ecol. Prog. Ser.*, 617-618, 277-294.

543 Collier, R., Edmond, J., 1984. The trace element geochemistry in marine biogenic particulate
544 matter. *Progr. Oceanogr.*, 13, 113-199.

545 Conway, T.M., John, S.G., 2014. The biogeochemical cycling of zinc and zinc isotopes in the
546 North Atlantic Ocean. *Glob. Biogeochem. cycles*, 28, 1111-1124.

547 Conway, T.M., Horner, T.J., Plancherel, Y., González, A.G., 2021. A decade of progress in
548 understanding cycles of trace elements and their isotopes in the oceans. *Chem. Geol.*, 580,
549 120381.

550 Coutaud, A., Meheut, M., Viers, J., Rols, J.-L., Pokrovsky, O. S., 2014. Zn isotope
551 fractionation during interaction with phototrophic biofilm. *Chem. Geol.*, 390, 46-60.

552 Cox, A., Saito, M.A., 2013. Proteomic responses of oceanic *Synechococcus* WH8102 to
553 phosphate and zinc scarcity and cadmium additions. *Front. Microbiol.*, 4, article 387.

554 Criss, R., 1999. Principle of stable isotope distribution. Oxford University Press, Oxford

555 Croot, P.L., Moffett, J.W., Brand, L.E., 2000. Production of extracellular Cu complexing
556 ligands by eukaryotic phytoplankton in response to Cu stress. *Limnol. Oceanogr.*, 45, 619-
557 627.

558 Cruzado, A., Velasquez, Z.R., 1990. Nutrients and phytoplankton in the Gulf of Lions,
559 northwestern Mediterranean. *Cont. Shelf Res.*, 9-11, 931-942.

560 Cullen, J., Sherrell, R.M., 1999. Techniques for determination of trace metals in small
561 samples of size-fractionated particulate matter: Phytoplankton metals off central
562 California. *Mar. Chem.*, 67, 233-247.

563 Damshäuser, A., Wagener, T., Garbe-Schönberg, D., Croot, P., 2013. Particulate and
564 dissolved aluminum and titanium in the upper water column of the Atlantic Ocean. *Deep-*
565 *Sea Res. I*, 73(C), 127-139.

566 Desaulty, A.M., Petelet-Giraud, EM., 2020. Zinc isotope composition as a tool for tracing
567 sources and fate of metal contaminants in rivers. *Sci. Tot. Environ.*, 728, 138599.

568 Desboeufs, K., Fu, F., Bressac, M., Tovar-Sánchez, A., Triquet, S., Doussin, J.-F., Giorio, C.,
569 Chazette, P., Disnaquet, J., Feron, A., Formenti, P., Maisonneuve, F., Rodríguez-Romero,
570 A., Zapf, P., Dulac, F., Guieu, C., 2022. Wet deposition in the remote western and central
571 Mediterranean as a source of trace metals to surface seawater. *Atmospheric Chemistry and*
572 *Physics*, 22, 2309–2332, <https://doi.org/10.5194/acp-22-2309-2022>.

573 Domsic, J.F., Avvaru, B.S., Kim, C.H., Gruner, S.M., Agbandje-McKenna, M., Silverman,
574 D.N., McKenna, R., 2008. Entrapment of Carbon Dioxide in the Active Site of Carbonic
575 Anhydrase II. *J. Biol. Chem.*, 283, 30766-30771.

576 Dong, S., Ochoa Gonzalez, R., Harrison, R.M., Green, D., North, R., Fowler, G., Weiss, D.,
577 2017. Isotopic signatures suggest important contributions from recycled gasoline, road dust
578 and non-exhaust traffic sources for copper, zinc and lead in PM10 in London, United
579 Kingdom. *Atmos. Environ.*, 165, 88-98.

580 Druce, M., Stirling, C.H., Rolinson, J.M., 2020. High-precision zinc isotopic measurement of
581 certified reference materials relevant to the environmental, earth, planetary and biomedical
582 sciences. *Geostand. Geoanalytical Res.*, 44, 711-732.

583 Ehrlich, S., Butler, I., Halicz, L., Rickard, D., Oldroyd, A., Matthews, A., 2004. Experimental
584 study of the copper isotope fractionation between aqueous Cu(II) and covellite, CuS.
585 Chem. Geol., 209, 259-269.

586 Fekiacova, Z., Cornu, S., Pichat, S., 2015. Tracing contamination sources in soils with Cu and
587 Zn isotopic ratios. Sci. Total Environ., 517, 96-105.

588 Fierro-González, P., Pagano, M., Guilloux, L., Makhoulouf, N., Tedetti, M., Carlotti F. 2022.
589 Zooplankton biomass, size structure, and associated metabolic fluxes with focus on its
590 roles at the chlorophyll maximum layer during the plankton-contaminant MERITE-
591 HIPPOCAMPE cruise. Mar. Pollut. Bul., submitted to this special issue.

592 Fujii, T., Moynier, F., Abe, M., Nemoto, K., Albarède, F., 2013. Copper isotope fractionation
593 between aqueous compounds relevant to low temperature geochemistry and biology.
594 Geochim. Cosmochim. Acta, 110, 29-44.

595 Gélabert, A., Pokrovsky, O.S., Viers, J., Schott, J., Boudou, A., Feurtet-Mazel, A., 2006.
596 Interaction between zinc and freshwater and marine diatom species: surface complexation
597 and Zn isotope fractionation. Geochim. Cosmochim. Acta, 70, 839-857.

598 Goni-Urriza, M., Moussard, H., Lafabrie, C., Carre, C., Bouvy, M., Sakka Hlaili, A.,
599 Pringault, O., 2018. Consequences of contamination on the interactions between
600 phytoplankton and bacterioplankton. Chemosphere, 195, 212-222.

601 Graham, S., Pearson, N., Jackson, S., Griffin, W., O'Reilly, S.Y., 2004. Tracing Cu and Fe
602 from source to porphyry: in situ determination of Cu and Fe isotope ratios in sulfides from
603 the Grasberg Cu–Au deposit. Chem. Geol., 207, 147-169.

604 Guieu, C., Loÿe- Pilot, M.D., Ridame, C., Thomas C. 2002. Chemical characterization of the
605 Saharan dust end- member: Some biogeochemical implications for the western
606 Mediterranean Sea, J. Geophys. Res., 107 (D15), 4258

607 Heimbürger, L.E., Mignon, C., Dufour, A., Chiffoleau, J.F., Cossa, D., 2010. Trace metal
608 concentrations in the North-western Mediterranean atmospheric aerosol between 1986 and
609 2008: Seasonal patterns and decadal trends. *Sci. Tot. Environ.*, 408, 2629-2638.

610 Heimbürger, L.E., Mignon, C., Cossa, D., 2011. Impact of atmospheric deposition of
611 anthropogenic and natural trace metals on Northwestern Mediterranean surface waters: A
612 box model assessment. *Environ. Pollut.*, 159, 1629-1634.

613 Ho, T.Y., Wen, L.S., You, C.F., Lee, D.C., 2007. The trace metal composition of size-
614 fractionated plankton in the South China Sea: Biotic versus abiotic sources. *Limnol.*
615 *Oceanogr.*, 52, 1776-1788.

616 Hulot, F.D., Lacroix, G., Lescher-Moutoué, F.O., Loreau, M., 2000. Functional diversity
617 governs ecosystem response to nutrient enrichment. *Nature*, 405, 340-344.

618 Jaouen, K., Pons, M.L., Balter, V., 2013. Iron, copper and zinc isotopic fractionation up
619 mammal trophic chains. *Earth Planet. Sci. Lett.*, 374, 164-172.

620 Jeandel, C., Rutgers van der Loeff, M., Lam, P.J., Roy-Barman, M., Sherrell, R.M.,
621 Kretschmer, S., German, C., Dehairs, F., 2015. What did we learn about ocean particle
622 dynamics in the GEOSECS–JGOFS era? *Progr. Oceanogr.*, 133, 6-16.

623 John, S. G., Conway, T.M., 2014. A role for scavenging in the marine biogeochemical cycling
624 of zinc and zinc isotopes. *Earth Planet. Sci. Lett.*, 394, 159-167.

625 John, S.G., Geis, R.W., Saito, M.A., Boyle, E.A., 2007a. Zinc isotope fractionation during
626 high affinity and low-affinity zinc transport by the marine diatom *Thalassiosira oceanica*.
627 *Limnol. Oceanogr.*, 52, 2710-2714.

628 John, S. G., Genevieve Park, J., Zhang, Z., Boyle, E. A., 2007b. The isotopic composition of
629 some common forms of anthropogenic zinc. *Chem. Geol.*, 245, 61–69.

630 Johnston, E.L., Roberts, D.A., 2009. Contaminants reduce the richness and evenness of
631 marine communities: a review and meta-analysis. *Environ. Pollut.*, 157, 1745-1752.

632 Juillot, F., Maréchal, C., Morin, G., Jouvin, D., Cacaly, S., Telouk, P., Benedetti, M.F.,
633 Ildefonse, P., Sutton, S., Guyot, F., Brown, G.E. Jr, 2011. Contrasting isotopic signatures
634 between anthropogenic and geogenic Zn and evidence for post depositional fractionation
635 processes in smelter-impacted soils from Northern France. *Geochim. Cosmochim. Acta*,
636 75, 2295-2305.

637 Lacoste, E., Raimbault, P., Harmelin-Vivien, M., Gaertner-Mazouni, N., 2016. Trophic
638 relationships between the farmed pearl oyster *Pinctada margaritifera* and its epibionts
639 revealed by stable isotopes and feeding experiments. *Aquacult. Environ. Interact.*, 8, 55-66.

640 Larson, P.B., Maher, K., Ramos, F.C., Chang, Z., Gaspar, M., Meinert, L., 2003. Copper
641 isotope ratios in magmatic and hydrothermal ore-forming environments. *Chem. Geol.*, 201,
642 337-350.

643 Lauer, M.M., Bianchini, A., 2010. Chronic copper toxicity in the estuarine copepod *Acartia*
644 *Tonsa* at different salinities. *Environ. Toxicol. Chem.*, 29, 2297-2303.

645 Lam, P.J., Lee, J.M., Heller, M.I., Mehic, S., Xiang, Y., Bates, N.R., 2018. Size-fractionated
646 distributions of suspended particle concentration and major phase composition from the
647 U.S. GEOTRACES Eastern Pacific Zonal Transect (GP16). *Mar. Chem.*, 201, 90-107.

648 Lemaitre, N., de Souza, G.F., Archer, C., Wang, R.M., Planquette, H., Sarthou, G., Vance, D.,
649 2020a. Pervasive sources of isotopically light zinc in the North Atlantic Ocean. *Earth*
650 *Planet. Sci. Lett.*, 539, 116216.

651 Liao, W.H., Yang, S.C., Ho, T.Y., 2017. Trace metal composition of size-fractionated
652 plankton in the Western Philippine Sea: The impact of anthropogenic aerosol deposition.
653 *Limnol. Oceanogr.*, 62, 2243-2259.

654 Little, S.H., Vance, D., Walker-Brown, C., Landing, W.M., 2014. The oceanic mass balance
655 of copper and zinc isotopes, investigated by analysis of their inputs, and outputs to
656 ferromanganese oxide sediments. *Geochim. Cosmochim. Acta*, 125, 673-693.

657 Little, S.H., Archer, C., Milne, A., Schlosser, C., Achterberg, E.P., Lohan, M.C., Vance, D.,
658 2018. Paired dissolved and particulate phase Cu isotope distributions in the South Atlantic.
659 Chem. Geol., 502, 29-43.

660 Liu, S.A., Huang, J., Liu, J., Wörner, G., Yang, W., Tang, Y.J., Chen, Y., Tang, L., Zheng, J.,
661 Li, S., 2015. Copper isotopic composition of the silicate Earth. Earth Planet. Sci. Lett., 427,
662 95-103.

663 Llamas-Dios, M.I., Vadillo, I., Jimenez-Gavilan, P., Candela, L., Corada-Fernandez, C., 2021.
664 Assessment of a wide array of contaminants of emerging concern in a Mediterranean water
665 basin (Guadalhorce river, Spain): Motivations for an improvement of water management
666 and pollutants surveillance. Science of the Total Environment, 788, 147822.

667 Luy, N., Gobert, S., Sartoretto, S., Biondo, R., Bouquegneau, J.M., Richir, J., 2012. Chemical
668 contamination along the Mediterranean French coast using *Posidonia oceanica* (L.) Delile
669 above-ground tissues: a multiple trace element study. Ecol. Indic., 18, 269-277.

670 Macias, D., Huertas, I.E., Garcia-Gorriz, E., Stips, A., 2019. Non-Redfieldian dynamics
671 driven by phytoplankton phosphate frugality explain nutrient and chlorophyll patterns in
672 model simulations for the Mediterranean Sea. Progr. Oceanogr., 173, 37-50.

673 Maher, K.C., Larson, P.B., 2007. Variation in copper isotope ratios and controls on
674 fractionation in hypogene skarn mineralization at Corocochuayco and Tintaya, Peru:
675 copper isotope ratios in magmatic and hydrothermal ore-forming environments. Econ.
676 Geol., 102, 225-237.

677 Marañón, E., Wambeke, F., Uitz, J., Boss, E., Dimier, C., Dinasquet, J., Engel, A., Haëntjens,
678 N., Pérez-Lorenzo, M., Taillandier, V., Zäncker, B., 2021. Deep maxima of phytoplankton
679 biomass, primary production and bacterial production in the Mediterranean Sea.
680 Biogeosciences, 18, 1749-1767.

681 Maréchal, C.N., 1998. Géochimie isotopique du cuivre et du zinc : méthode, variabilité
682 naturelle et application océanographique. Thèse Univ J. Fourier, Grenoble I (France),
683 260pp.

684 Maréchal, C.N., Telouk, P., Albarède, F., 1999. Precise analysis of copper and zinc isotopic
685 composition by plasma-source mass spectrometry. *Chem. Geol.*, 156, 251-273.

686 Maréchal, C.N., Nicolas, E., Douchet, C., Albarède, F., 2000. Abundance of zinc isotopes as a
687 marine biogeochemical tracer. *Geochem. Geophys.*, 1, 1-15.

688 Maréchal, C., Albarède, F., 2002. Ion-exchange fractionation of copper and zinc isotopes.
689 *Geochim. Cosmochim. Acta*, 66, 1499-1509.

690 Mason, T.F.D., Weiss, D.J., Chapman, J.B., Wilkinson, J.J., Tessalina, S.G., Spiro, B.,
691 Horstwood, M.S.A., Spratt, J., Coles, B.J., 2005. Zn and Cu isotopic variability in the
692 Alexandrinka volcanic-hosted massive sulphide (VHMS) ore deposit, Urals, Russia. *Chem*
693 *Geol.*, 221, 170-187.

694 Mathur, R., Ruiz, J., Titley, S., Liermann, L., Buss, H., Brantley, S., 2005. Cu isotopic
695 fractionation in the supergene environment with and without bacteria. *Geochim.*
696 *Cosmochim. Acta*, 69, 5233-5246.

697 Mathur, R., Munk, L.A., Townley, B., Gou, K.Y., Gómez Miguélez, N., Titley, S., Chen,
698 G.G., Song, S., Reich, M., Tornos, F., Ruiz, J., 2014. Tracing low-temperature aqueous
699 metal migration in mineralized watersheds with Cu isotope fractionation. *Appl. Geochem.*,
700 51, 109-115.

701 The MerMex Group, 2011. Marine ecosystems' responses to climatic and anthropogenic
702 forcings in the Mediterranean. *Progress in Oceanography*, 91, 97-166.

703 Micheli, F., Halpern, B.S., Walbridge, S., Ciriaco, S., Ferretti, F., Fraschetti, S., Lewison, R.,
704 Nykjaer, L., Rosenberg, A.A., 2013. Cumulative Human Impacts on Mediterranean and

705 Black Sea Marine Ecosystems: Assessing Current Pressures and Opportunities. PLOS One,
706 8, e79889.

707 Moffett, J.W., Zika, R.G., Brand, L.E., 1990. Distribution and potential sources and sink of
708 copper chelators in the Sargasso Sea. *Deep Sea Res. (A)*, 37, 27-36.

709 Moffett, J.W., Brand, L.E., 1996. Production of strong, extracellular Cu chelators by marine
710 cyanobacteria in response to Cu stress. *Limnol. Oceanogr.*, 41, 388-395.

711 Moffett, J.W., Brand, L.E., Croot, P.L., Barbeau, K.A., 1997. Cu speciation and
712 cyanobacterial distribution in harbors subject to anthropogenic Cu inputs. *Limnol
713 Oceanogr.*, 42, 789-799.

714 Morel, M.M., Price, N.M., 2003. Biogeochemical cycles of trace metals in the oceans.
715 *Science*, 300, 944-947.

716 Morel, F.M.M., 2008. The co-evolution of phytoplankton and trace element cycles in the
717 oceans. *Geobiol.*, 6, 318-324.

718 Moynier, F., Vance, D., Fujii, T., Savage, P., 2017. The Isotope Geochemistry of Zinc and
719 Copper. *Rev. Mineral. Geochem.*, 82, 543-600.

720 Navarrete, J., Borrok, D., Viveros, M., Ellzey, J., 2011. Copper isotope fractionation during
721 surface adsorption and intracellular incorporation by bacteria. *Geochim. Cosmochim. Acta*,
722 75, 784-799.

723 Ohnemus, D., Lam, P.J., 2015. Cycling of lithogenic marine particles in the US
724 GEOTRACES North Atlantic transect. *Deep-Sea Res. II*, 116, 283-302.

725 Oursel, B., Garnier, C., Durrieu, G., Mounier, S., Omanović, D., Lucas, Y., 2013. Dynamics
726 and fates of trace metals chronically input in a Mediterranean coastal zone impacted by a
727 large urban zone. *Mar. Pollut. Bull.*, 69, 137-149.

728 Peel, K., Weiss, D., Sigg, L., 2009. Zinc isotope composition of settling particles as a proxy
729 for biogeochemical processes in lakes: Insights from the eutrophic Lake Greifen,
730 Switzerland, *Limnol. Oceanogr.*, 54, 1699-1708.

731 Peers, G., Quesnel, S.A., Price, N.M., 2005. Copper requirements for iron acquisition and
732 growth of coastal and oceanic diatoms. *Limnol. Oceanogr.*, 50, 1149-1158.

733 Peers, G., Price, N. M., 2006. Copper-containing plastocyanin used for electron transport by
734 an oceanic diatom. *Nature*, 441, 341-344.

735 Petit, J.C.J., de Long, J., Chou, L., Mattielli, N., 2008. Development of Cu and Zn isotope
736 MC-ICP-MS measurements: application to suspended particulate matter and sediments
737 from the Scheldt estuary. *Geostand. Geoanalytical Res.*, 32, 149-166.

738 Pey, J., Pérez, N., Querol, X., Alastuey, A., Cusack, M., Reche, C., 2010. Intense winter
739 atmospheric pollution episodes affecting the Western Mediterranean. *Sci. Tot. Environ.*,
740 408, 1951-1959.

741 Planquette, H., Sherrell, R.M., 2012. Sampling for particulate trace element determination
742 using water sampling bottles: methodology and comparison to in situ pumps. *Limnol.*
743 *Oceanogr. Methods*, 10, 367-388.

744 Pringault, O., Bouvy, M., Carre, C., Fouilland, E., Meddeb, M., Mejri, K., Leboulanger, C.,
745 Hlaili, A.S., Sakka Hlaili, A., 2020. Impacts of chemical contamination on bacterio-
746 phytoplankton coupling. *Chemosphere*, 257, 127165.

747 Pringault, O., Bouvy, M., Carre, C., Mejri, K., Bancon-Montigny, C., Gonzalez, C.,
748 Leboulanger, C., Hlaili, A.S., Goni-Urriza, M., 2021. Chemical contamination alters the
749 interactions between bacteria and phytoplankton. *Chemosphere*, 278, 130457.

750 Quéméneur, M., Lajnef, R., Cabrol, L., Mission, B., Tedetti, M., Chifflet, S., Belhassen, M.,
751 Bellaj Zouari, A., 2022. Prokaryotic diversity within various size-fractions of plankton and

752 associated contaminants along a North-South Mediterranean transect. *Mar. Pollut. Bull.*, in
753 prep in this special issue.

754 Radakovich, O., Roussiez, V., Ollivier, P., Ludwig, W., Grenz, C., Probst, J.L., 2008.
755 Particulate heavy metals input from rivers and associated sedimentary deposits on the Gulf
756 of Lion continental shelf. *Estuar. Coast. Shelf Sci.*, 77, 285-295.

757 Raimbault P., Garcia, N., 2008. Evidence for efficient regenerated production and dinitrogen
758 fixation in nitrogen-deficient waters of the South Pacific Ocean: impact on new and export
759 production estimates. *Biogeosciences*, 5, 323-338.

760 Rouxel, O., Fouquet, Y., Ludden, J.N., 2004. Copper Isotope Systematics of the Lucky Strike,
761 Rainbow, and Logatchev Sea-Floor Hydrothermal Fields on the Mid-Atlantic Ridge.
762 *Chem. Geol.*, 99, 585-600.

763 Rossi, N., Jamet, J.L., 2008. In situ heavy metals (copper, lead and cadmium) in different
764 plankton compartments and suspended particulate matter in two coupled Mediterranean
765 coastal ecosystems (Toulon bay, France). *Mar. Pollut. Bull.*, 56, 1862-1870.

766 Rue, E., Bruland, K., 2001. Domoic acid binds iron and copper: a possible role for the toxin
767 produced by the marine diatom *Pseudo-nitzschia*. *Mar. Chem.*, 76, 127-134.

768 Ryan, B.M., Kirby, J.K., Degryse, F., Scheiderich, K., McLaughlin, M.J., 2014. Copper
769 isotope fractionation during equilibration with natural and synthetic ligands. *Environ. Sci.*
770 *Technol.*, 48, 8620-8626.

771 Schleicher, N., Dong, S., Packman, H., Little, S.H., Ochoa Gonzales R., Najorka, J., Sun, Y.,
772 Weiss, D.J., 2020. A global assessment of copper, zinc and lead isotopes in mineral dust
773 sources and aerosols. *Front. Earth Sci.*, 8, 167.

774 Shaked, Y., Xu, Y., Leblanc, K., Morel, M.M., 2006. Zinc availability and alkaline
775 phosphatase activity in *Emiliania huxleyi*: Implications for Zn-P co-limitation in the ocean.
776 *Limnol. Oceanogr.*, 51, 299-309.

777 Shield, A.E., Weis, D., Orians, K.J., 2010. Evaluation of zinc, cadmium and lead isotope
778 fractionation during smelting and refining. *Sci. Tot. Environ.*, 408, 2357-2368.

779 Sivry, Y., Riotte, J., Sonke, J.E., Audry, S., Schäfer, J., Viers, J., Blanc, G., R. Freydier, R., .
780 Dupré B., 2008. Zn isotopes as tracers of anthropogenic pollution from Zn-ore smelters
781 The Riou Mort–Lot River system. *Chem. Geol.*, 255, 295-304.

782 Sonke, J.E., Sivry, Y., Viers, J., Freydier, R., Dejonghe, L., André, L., Aggarwal, J.K.,
783 Fontan, F., Dupré, B., 2008. Historical variations in the isotopic composition of
784 atmospheric zinc deposition from a zinc smelter. *Chem. Geol.*, 252, 145-157

785 Souto-Oliviera, C.E., Babinski, M., Araújo, D., Andrade, M.F., 2018. Multi-isotopic
786 fingerprints (Pb, Zn, Cu) applied for urban aerosol source apportionment and
787 discrimination. *Sci. Tot. Environ.*, 626, 1350-1366.

788 Souto-Oliviera, C.E., Babinski, M., Araújo, D., Weiss, D.J., Ruiz, I.R., 2019. Multi-isotope
789 approach of Pb, Cu and Zn in urban aerosols and anthropogenic sources improves tracing
790 of the atmospheric pollutant sources in megacities. *Atmos. Environ.*, 198, 427-437.

791 Sunda, W., 2012. Feedback interactions between trace metal nutrients and phytoplankton in
792 the ocean. *Front. Microbiol.*, 3, 204.

793 Takano, S., Liao, W.H., Tian, H.A., Huang, K.F., Ho, T.Y., Sohrin, Y., 2020. Source of
794 particulate Ni and Cu in the water column of the northern South China Sea: evidence from
795 elemental and isotope ratios in aerosols and sinking particles. *Mar. Chem.*, 219, 103751.

796 Tedetti, M., Tronczynski, J., 2019. HIPPOCAMPE cruise, RV Antea.
797 <https://doi.org/10.17600/18000900>

798 Tedetti, M., Tronczynski, J., Carlotti, F., Pagano, M., Sammari, C., Bel Hassen, M., Ben
799 Ismail, S., Desboeufs, K., Poindron, C., Chifflet, S., Abdennadher, M., Amri, S., Bănarua,
800 D., Ben Abdallah, L., Bhairy, N., Boudriga, I., Bourin, A., Brach-Papa, C., Briant, N.,
801 Cabrol, L., Chevalier, C., Chouba, L., Coudray, S., Daly Yahia, M.N., de Garidel-Thoroni

802 T., Dufour, A., Dutay, J.-C., Espinasse, B., Fierro, P., Fornier, M., Garcia, N., Giner, F.,
803 Guigue, C., Guilloux, L., Hamza, A., Heimbürger-Boavida, L.-E., Jacquet, S., Knoery, J.,
804 Lajnef, R., Makhoulouf Belkahia, N., Malengros, D., Martinot, P.L., Bosse, A., Mazur, J.-C.,
805 Meddeb, M., Misson, B., Pringault, O., Quéméneur, M., Radakovitch, O., Raimbault, P.,
806 Ravel, C., Rossi, V., Rwawi, C., Sakka Hlaili, A., Tesán Onrubia, J.A., Thomas, B.,
807 Thyssen, M., Zaaboub, N., Zouari, A., Garnier, C., 2022. Contamination of planktonic
808 food webs in the Mediterranean Sea: Setting the frame for MERITE-HIPPOCAMPE
809 oceanographic cruise (spring 2019). *Mar. Pollut. Bull.*, submitted to this special issue.

810 Tesán Onrubia, J.A., Tedetti, M., Carlotti, F., Tenaille, M., Guilloux, L., Pagano, M.,
811 Lebreton, B., Guillou, G., Fierro-Gonzalez, P., Guigue, C., Chifflet, S., Garcia, T.,
812 Boudriga, I., Belhassen, M., Zouari, A., Bănaru, D. Spatial variations of stable isotope
813 ratios and biochemical content of size-fractionated plankton in the Mediterranean Sea
814 (MERITE-HIPPOCAMPE campaign). *Mar. Pollut. Bull.*, submitted to this special issue.

815 UNEP/MAP-RAC-SPA, 2008. Impact of climate change on biodiversity in the Mediterranean
816 Sea. In: Perez T., RAC/SPA (Eds.), Tunis, 1-61.

817 Wiederhold, J.G., 2015. Metal stable isotope signatures as tracers in environmental
818 geochemistry. *Environ. Sci. Technol.*, 49, 2606-2624.

819 Yang, S.C., Hawco, N.J., Pinedo-Gonzales, P., Bian, X., Huang, K.F., Zhang, R., John, S.G.,
820 2020. A new purification method for Ni and Cu stable isotopes in seawater provides
821 evidence for widespread Ni isotope fractionation by phytoplankton in the North Pacific.
822 *Chem. Geol.*, 547, 119662.

823 Zhao, Y., Vance, D., Abouchami, W., de Baar, H.J.W., 2014. Biogeochemical cycling of zinc
824 and its isotopes in the Southern Ocean. *Geochim. Cosmochim. Acta*, 125, 653-672.

825 Zhao, D., Cao, X., Huang, R., Zeng, J., Wu, Q.L., 2017. Variation of bacterial communities in
826 water and sediments during the decomposition of *Microcystis* biomass. Plos One, 12,
827 e0176397.

828 Zhu, X. K., Guo, Y., Williams, R. J. P., O'nions, R. K., Matthews, A., Belshaw, N. S.,
829 Salvato, B., 2002. Mass fractionation processes of transition metal isotopes. Earth Planet.
830 Sci. Lett., 200, 47-62.

831 Zumft, W.G., Kroneck, P.M.H., 2007. Respiratory transformation of nitrous oxide (N₂O) to
832 dinitrogen by Bacteria and Archaea. Adv. Microb. Physiol., 52, 107-225.

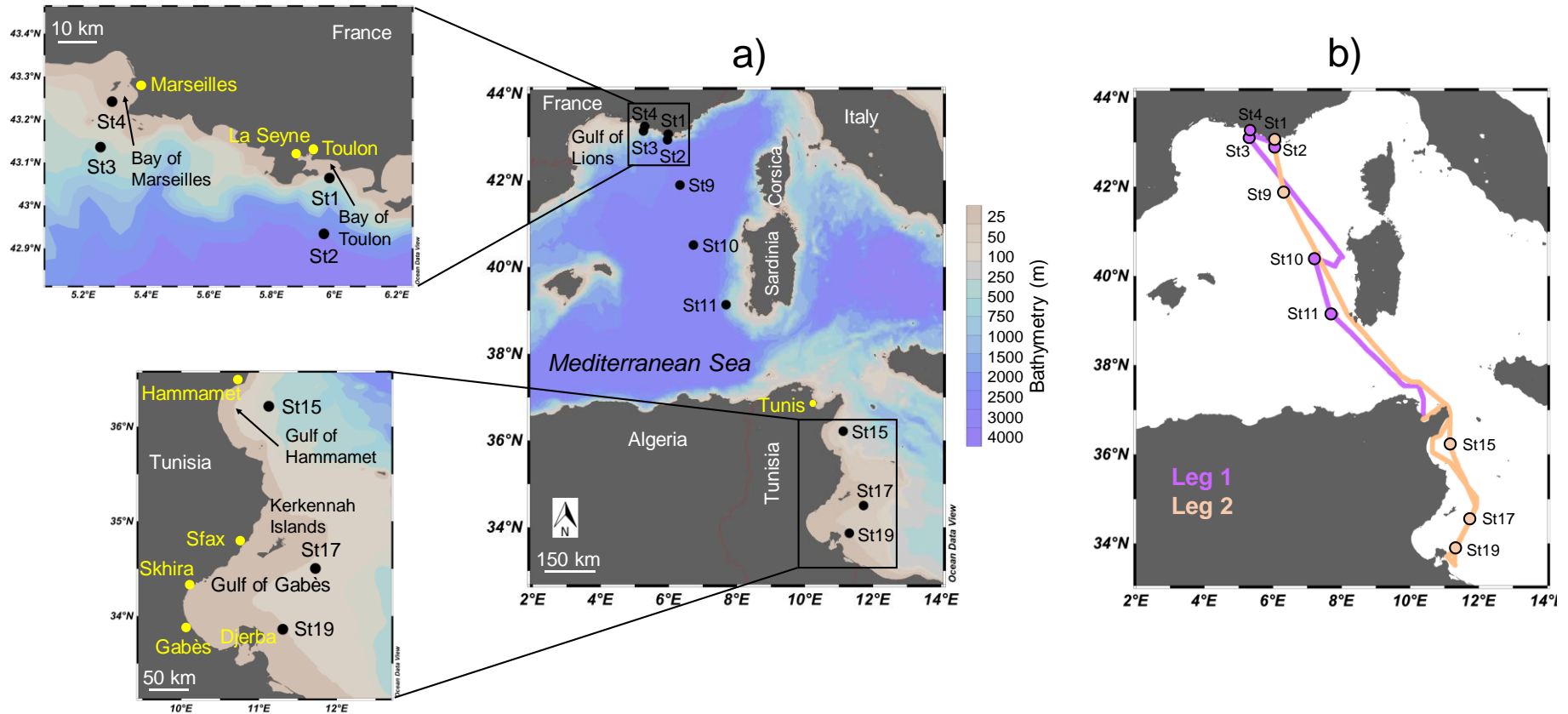


Figure 1. a) Location of the sampling stations in the Mediterranean Sea. b) Details of the MERITE-HIPPOCAMPE campaign tracks: Leg 1 (from La Seyne-sur-Mer to Tunis) with five sampling stations (St2, St4, St3, St10 and St11, in this chronological order); Leg 2 (from Tunis to Gulf of Gabès to La Seyne-sur-Mer) with five sampling stations (St15, St17, St19, St9 and St1, in this chronological order).

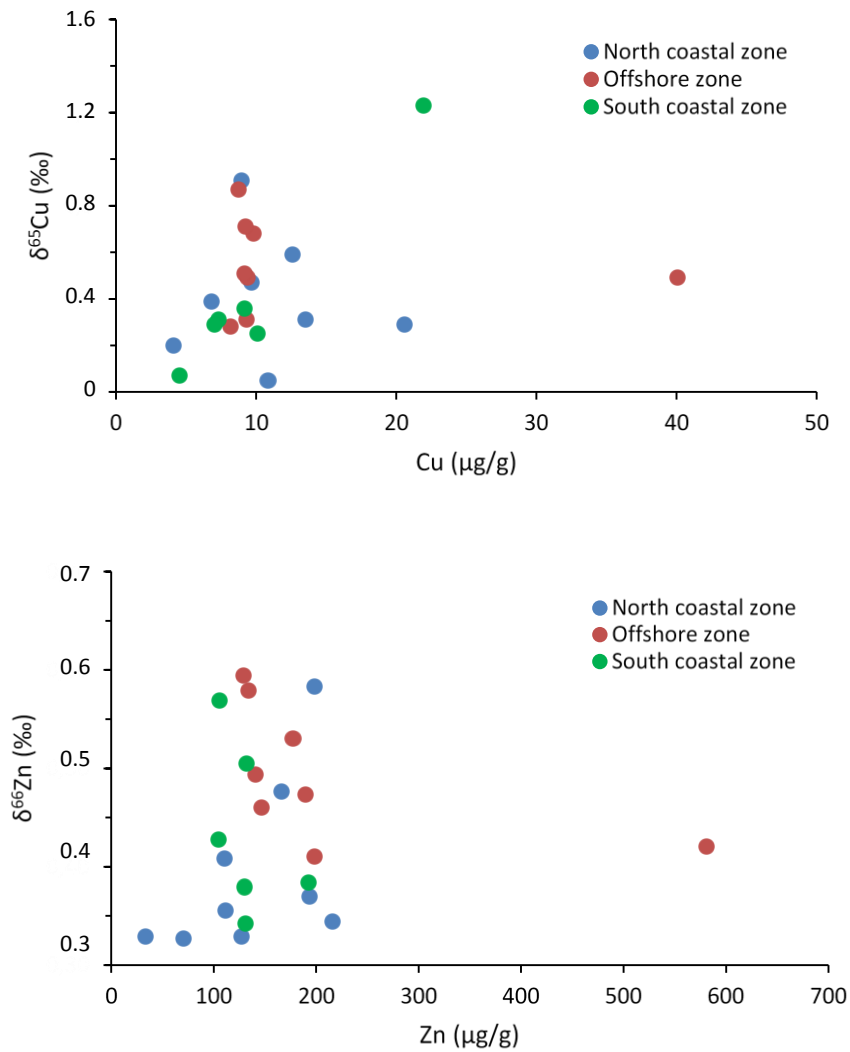


Figure 2. $\delta^{65}\text{Cu}$ and $\delta^{66}\text{Zn}$ variations relative to Cu and Zn concentrations in the four size fractions plankton (F3: 60–200, F4: 200–500, F5: 500–1000 and F6: 1000–2000 μm), respectively. Isotopic compositions are in ‰ and concentrations in $\mu\text{g/g}$ of dry sample. Values are grouped according to three geographical zones: the northern coastal zone (blue), the offshore zone (red) and the southern coastal zone (green).

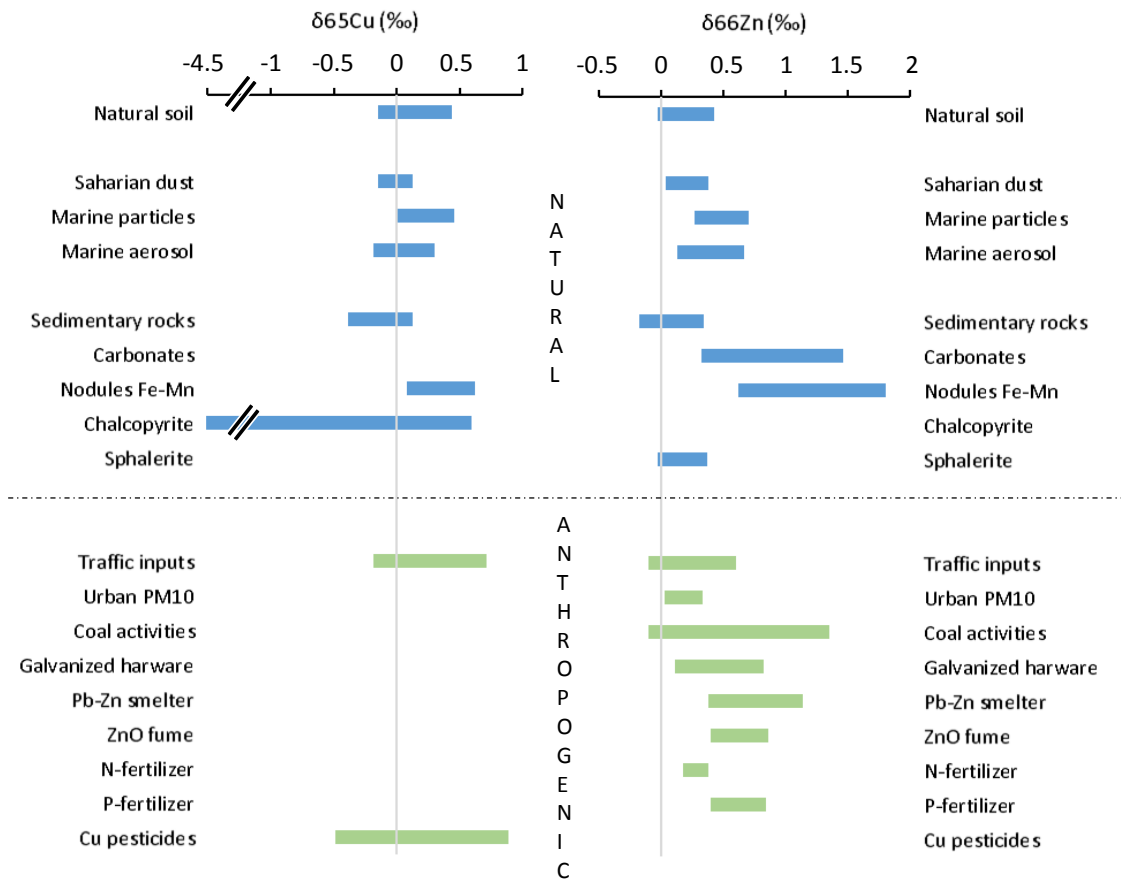


Figure 3. Summary of various $\delta^{65}\text{Cu}$ and $\delta^{66}\text{Zn}$ compositions in geogenic (natural and anthropogenic) sources.

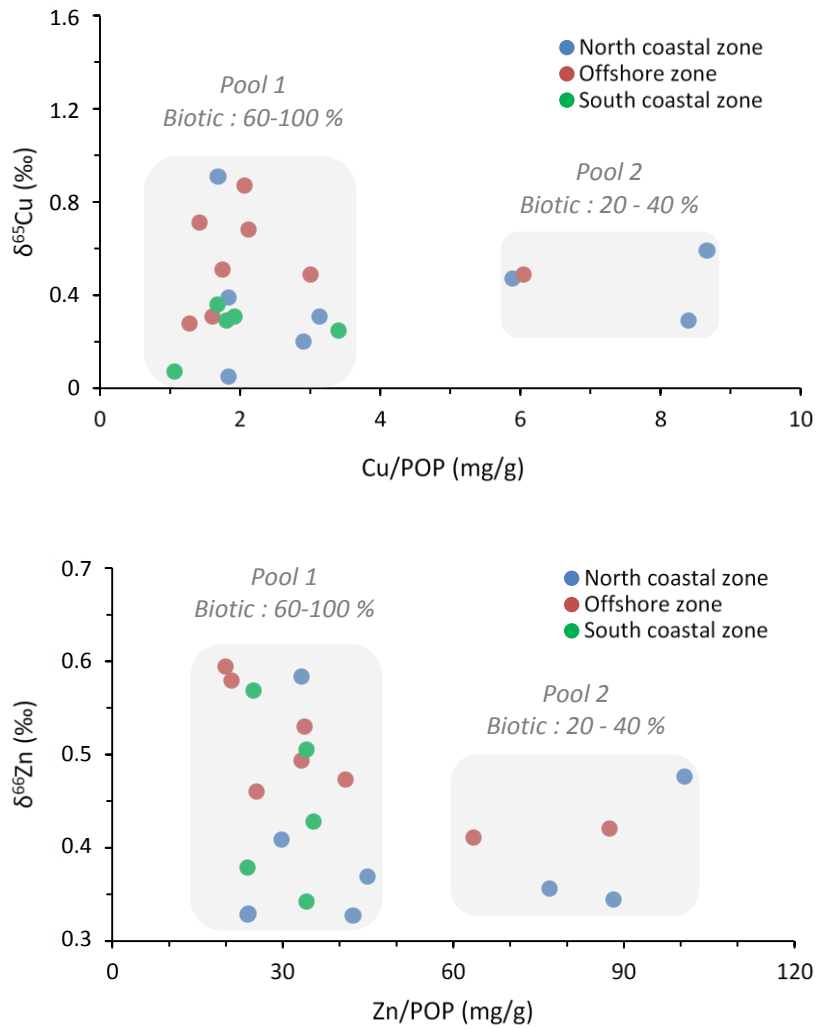


Figure 4. $\delta^{65}\text{Cu}$ and $\delta^{66}\text{Zn}$ variations relative to their corresponding Cu/POP and Zn/POP ratios in the four size fractions plankton (F3: 60–200, F4: 200–500, F5: 500–1000 and F6: 1000–2000 μm). Values are grouped according to three geographical zones: the northern coastal zone (blue), the offshore zone (red) and the southern coastal zone (green).

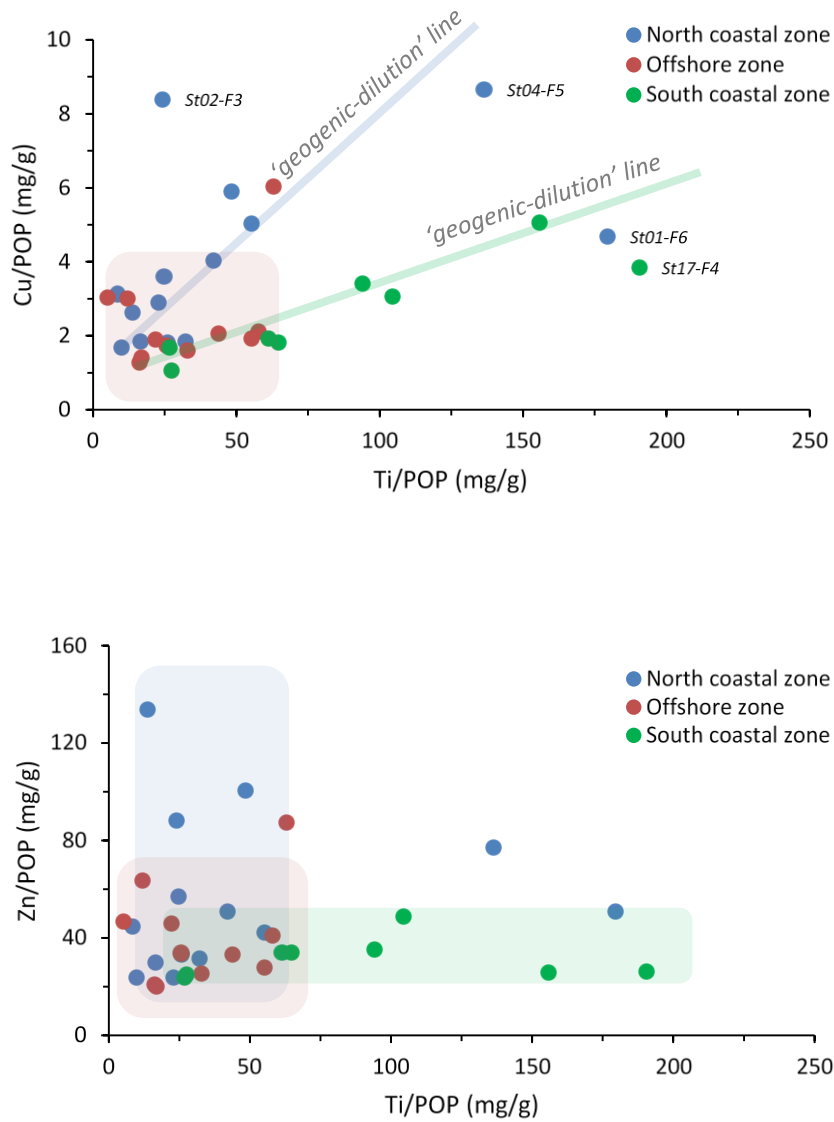


Figure 5. Cu/POP vs Ti/POP and Zn/POP vs Ti/POP diagrams in the four size fractions plankton (F3: 60–200, F4: 200–500, F5: 500–1000 and F6: 1000–2000 μm). Values are grouped according to three geographical zones: the northern coastal zone (blue), the offshore zone (red) and the southern coastal zone (green).

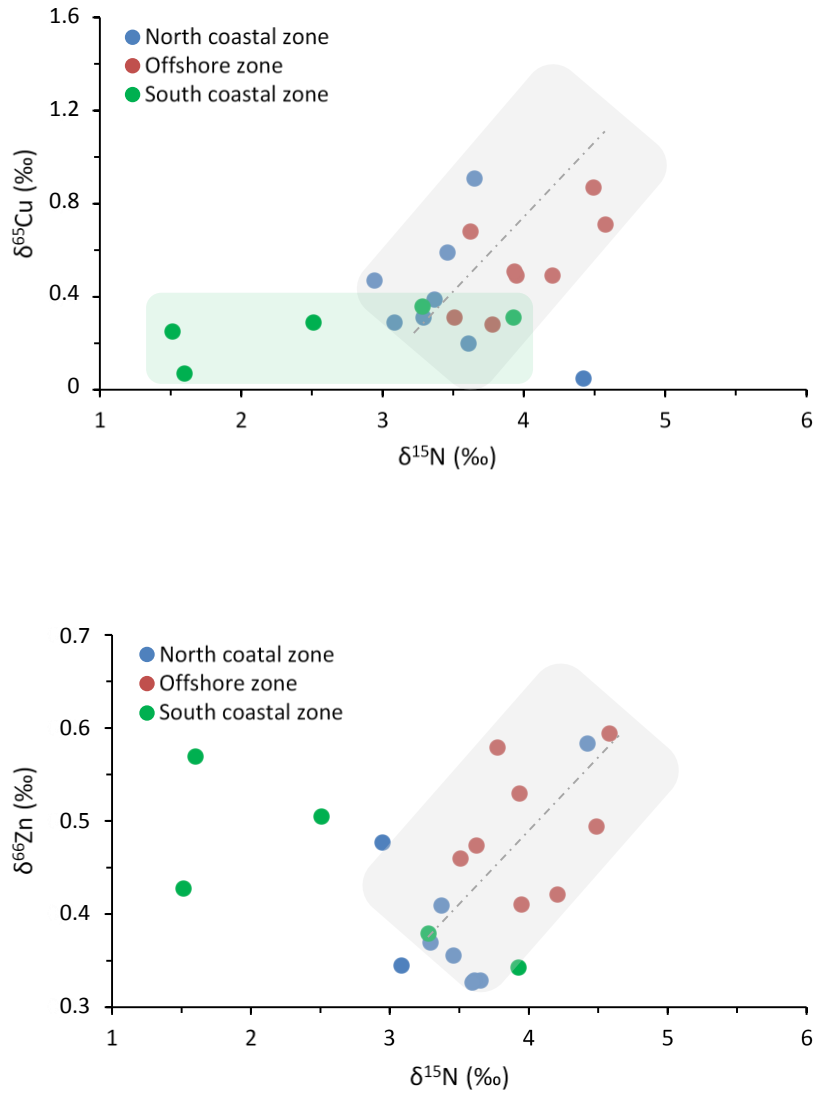


Figure 6. $\delta^{65}\text{Cu}$ and $\delta^{66}\text{Zn}$ variations relative to their corresponding $\delta^{15}\text{N}$ in the four size fractions plankton (F3: 60–200, F4: 200–500, F5: 500–1000 and F6: 1000–2000 μm). Isotopic compositions are in ‰. Values are grouped according to three geographical zones: the northern coastal zone (blue), the offshore zone (red) and the southern coastal zone (green).

Table 1. General information about the 10 stations sampled during the MERITE-HIPPOCAMPE campaign (April 13-May 14, 2019) aboard the *R/V Antea*.

Station	Latitude (N)	Longitude (E)	Localisation	Depth (m)	DCM (m)	Characteristics
St1	43°03.819'	5°59.080'	Toulon	91	20	Urbanized bay; intermittently bloom area
St2	42°56.020'	5°58.041'	Toulon	1770	25	Limit of continental shelf; intermittently bloom area
St3	43°08.150'	5°15.280'	Marseilles	95	55	Southeast entrance to the Gulf of Lions; intermittently bloom area
St4	43°14.500'	5°17.500'	Marseilles	58	31	Urbanized bay; intermittently bloom area
St9	41°53.508'	6°19.998'	Offshore	2575	20	North of the Balearic Thermal Front; Bloom area
St10	40°18.632'	7°14.753'	Offshore	2791	50	South of the Balearic Thermal Front; intermittently bloom area
St11	39°07.998'	7°41.010'	Offshore	1378	40	Algerian ecoregion; no bloom area
St15	36°12.883'	11°07.641'	Gulf of Hammamet	100	66	Near Sicily channel; No bloom area and high density of small pelagic fishes
St17	34°30.113'	11°43.573'	Gulf of Gabes	48	40	Gabès ecoregion; coastal bloom area, high density of small pelagic fishes
St19	33°51.659'	11°18.509'	Gulf of Gabes	50	40	Gabès ecoregion; coastal bloom area, high density of small pelagic fishes

Table 2. Multiparametric values obtained during the MERITE HIPPOCAMPE campaign (spring 2019) in the four planktonic size fractions (F3: 60-200 μm ; F4: 200-500 μm ; F5: 500-1000 μm ; F6: 1000-2000 μm) and the 10 stations (St1-4, St9-11, St15, St17, St19). Details of trace metal (Ti, $\mu\text{g/g}$), particulate organic phosphorus (POP, mg/g) and biotic component (Biotic, %) were presented in [Chifflet et al \(2022\)](#) and, details of nitrogen isotopic compositions ($\delta^{15}\text{N}$, ‰) were presented in [Tésan-Onrubia et al. \(2022\)](#) as companion papers.

Station	Fraction	Biotic (%)	Ti ($\mu\text{g/g}$)	POP (mg/g)	$\delta^{15}\text{N}$ (‰)
<i>Northern coastal zone (Marseilles-Toulon bays)</i>					
St01	F3	68	150.3	4.67	3.20
St01	F4	83	52.7	5.32	3.65
St01	F5	67	153.9	5.94	4.42
St01	F6	35	445.1	2.48	4.26
St02	F3	43	59.1	2.45	3.09
St02	F4	98	36.7	4.31	3.29
St02	F5	81	93.6	3.78	3.48
St02	F6	81	132.6	3.16	3.52
St03	F3	30	79.5	1.64	2.94
St03	F4	42	54.8	3.97	3.39
St03	F5	93	61.6	3.71	3.37
St03	F6	-	-	3.17	3.34
St04	F3	70	32.3	1.40	3.61
St04	F4	40	91.9	1.67	3.60
St04	F5	22	197.6	1.45	3.46
St04	F6	-	243.1	-	-
<i>Offshore zone (near the Balearic Thermal Front and the Algerian ecoregion)</i>					
St09	F3	100	59.4	2.70	1.99
St09	F4	98	16.5	3.19	2.73
St09	F5	90	37.6	3.11	3.95
St09	F6	-	37.8	-	-
St10	F3	74	267.0	4.61	3.62
St10	F4	90	133.9	5.24	3.94
St10	F5	84	186.2	4.24	4.49
St10	F6	89	274.7	4.98	5.67
St11	F3	80	191.1	5.80	3.51
St11	F4	89	103.7	6.39	3.78
St11	F5	23	417.4	6.64	4.20
St11	F6	85	110.4	6.48	4.58
<i>Southern coastal zone (Gulf of Gabès)</i>					
St15	F3	66	316.0	3.03	3.56

St15 F4	83	234.9	3.83	3.93
St15 F5	88	146.1	5.47	3.28
St15 F6	-	264.5	-	-
St17 F3	61	178.1	1.14	1.86
St17 F4	64	290.3	1.52	2.41
St17 F5	-	590.4	-	-
St17 F6	-	-	-	-
St19 F3	60	278.6	2.96	1.51
St19 F4	97	116.5	4.26	1.60
St19 F5	-	251.6	3.88	2.51
St19 F6	-	842.9	-	-

Table 3. Concentrations ($\mu\text{g/g}$) and isotopic compositions (‰) of Cu and Zn in four planktonic size fractions (F3: 60-200 μm ; F4: 200-500 μm ; F5: 500-1000 μm ; F6: 1000-2000 μm) collected at the deep chlorophyll maximum (DCM) according to three geographical areas (the northern coastal zone, the offshore zone, and the southern coastal zone).

Station	Fraction	Cu ($\mu\text{g/g}$)	Zn ($\mu\text{g/g}$)	$\delta^{65}\text{Cu}$ (‰)	$2\sigma_{\text{Cu}}$ (‰)	$\delta^{66}\text{Zn}$ (‰)	$2\sigma_{\text{Zn}}$ (‰)
<i>Northern coastal zone (Marseilles-Toulon bays)</i>							
St1	F3	8.63	148.10	-	-	-	-
St1	F4	8.95	126.70	0.91	0.02	0.33	0.03
St1	F5	10.85	197.97	0.05	0.01	0.58	0.03
St1	F6	11.60	125.54	-	-	-	-
St2	F3	20.57	216.00	0.29	0.01	0.34	0.03
St2	F4	13.49	193.30	0.31	0.09	0.37	0.03
St2	F5	13.58	214.78	-	-	-	-
St2	F6	12.81	160.32	-	-	-	-
St3	F3	9.69	165.67	0.47	0.01	0.48	0.04
St3	F4	10.42	530.69	-	-	-	-
St3	F5	6.82	110.16	0.39	0.06	0.41	0.03
St3	F6	-	-	-	-	-	-
St4	F3	4.07	33.63	0.2	0.06	0.33	0.03
St4	F4	8.37	70.51	-	-	0.33	0.02
St4	F5	12.55	111.47	0.59	0.01	0.36	0.03
St4	F6	16.99	149.42	-	-	-	-
<i>Offshore zone (near the Balearic Thermal Front and the Algerian ecoregion)</i>							
St9	F3	5.14	124.11	-	-	-	-
St9	F4	9.65	149.54	-	-	-	-
St9	F5	9.36	197.92	0.49	0.03	0.41	0.03
St9	F6	7.50	132.38	-	-	-	-
St10	F3	9.81	189.76	0.68	0.00	0.47	0.04
St10	F4	9.14	177.28	0.51	0.07	0.53	0.04
St10	F5	8.76	141.08	0.87	0.06	0.49	0.04
St10	F6	9.59	139.39	-	-	-	-
St11	F3	9.32	147.16	0.31	0.02	0.46	0.04
St11	F4	8.17	133.56	0.28	0.02	0.58	0.04
St11	F5	40.09	580.68	0.49	0.02	0.42	0.03
St11	F6	9.21	129.32	0.71	0.02	0.59	0.03
<i>Southern coastal zone (Gulf of Gabès)</i>							
St15	F3	9.28	148.03	-	-	-	-
St15	F4	7.33	130.82	0.31	0.02	0.34	0.02
St15	F5	9.14	130.38	0.36	0.01	0.38	0.03

St15	F6	8.18	108.30	-	-	-	-
St17	F3	5.81	29.63	-	-	-	-
St17	F4	5.85	39.70	-	-	-	-
St17	F5	21.92	192.53	1.23	0.01	0.38	0.04
St17	F6	-	-	-	-	-	-
St19	F3	10.08	104.96	0.25	0.05	0.43	0.04
St19	F4	4.52	105.83	0.07	0.01	0.57	0.04
St19	F5	7.02	132.35	0.29	0.01	0.51	0.04
St19	F6	5.62	67.74	-	-	-	-
